

Old Dominion University

ODU Digital Commons

Electrical & Computer Engineering Theses & Dissertations

Electrical & Computer Engineering

Summer 2009

Analysis of Partial Discharge Pulse Height Distribution Parameters

Vinay N. Nimbole
Old Dominion University

Follow this and additional works at: https://digitalcommons.odu.edu/ece_etds



Part of the [Artificial Intelligence and Robotics Commons](#), [Electrical and Electronics Commons](#), [Numerical Analysis and Scientific Computing Commons](#), and the [Theory and Algorithms Commons](#)

Recommended Citation

Nimbole, Vinay N.. "Analysis of Partial Discharge Pulse Height Distribution Parameters" (2009). Master of Science (MS), Thesis, Electrical & Computer Engineering, Old Dominion University, DOI: 10.25777/3dg5-z743
https://digitalcommons.odu.edu/ece_etds/460

This Thesis is brought to you for free and open access by the Electrical & Computer Engineering at ODU Digital Commons. It has been accepted for inclusion in Electrical & Computer Engineering Theses & Dissertations by an authorized administrator of ODU Digital Commons. For more information, please contact digitalcommons@odu.edu.

ANALYSIS OF PARTIAL DISCHARGE PULSE HEIGHT DISTRIBUTION PARAMETERS

by

Vinay N. Nimbole

B.Tech., April 2006, Jawaharlal Nehru Technological University, India

A Thesis Submitted to the Faculty of
Old Dominion University in Partial Fulfillment of the
Requirements for the Degree of

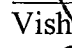
MASTER OF SCIENCE

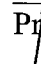
ELECTRICAL ENGINEERING


OLD DOMINION UNIVERSITY

August 2009

Approved by:


Vishnukumar K. Lakdawala (Director)


Prathap Basappa (Member)


Linda Vahala (Member)

ABSTRACT

ANALYSIS OF PARTIAL DISCHARGE PULSE HEIGHT DISTRIBUTION PARAMETERS

Vinay N. Nimbole
Old Dominion University, August 2009
Director: Dr. Vishnu K. Lakdawala

Partial Discharges (PD) have been traditionally used to assess the state of any insulation system and its remnant life. In earlier work, Perspex (PMMA) samples with a needle plane gap have been aged with AC voltage. Their tree growth was monitored simultaneously by collecting PD at regular intervals of time and taking microphotographs in real time without interrupting the aging voltage. The obtained partial discharge pulse amplitude records were clustered together into groups of class intervals. The sequence of PD pulse height records was quantified as a time series of shape (η), and scale (σ) parameters of a Weibull distribution. This thesis describes two new techniques to analyze and predict the pulse height distribution parameters of PD (η and σ): Linear prediction and artificial neural networks. To test these techniques, we have analyzed the experimental results for the two samples of data previously obtained. Simulation results in MATLAB show that both methods predict the future values of each sample with optimal mean square errors. The relative advantages and limitations of each approach are discussed. A state of the art experimental system to conduct PD measurements and analysis was built as part of the present work. This system will be used for future research work.

Copyright © 2009, by Vinay N. Nimbole. All Rights Reserved.

Dedicated to my grandmother, *Aai*.

Thank you for your unconditional love and blessings.

ACKNOWLEDGMENT

I wish to express my heartfelt gratitude to Dr. Vishnu K Lakdawala for giving me the enriching and rewarding opportunity of being a part of his research team. It is only through his constant guidance, encouragement and support that this work has been possible.

I wish to thank Dr. Basappa for introducing me to the amazing world of Partial Discharge through his IDEL lab and also for familiarizing me with the concepts that have been extremely instrumental in the final outcome of this thesis work.

I would like to thank my family – Dad, Mom, Priya (Sister), Vikram (Brother-in-Law) for showering unconditional love on me and believing in me. Finally, I would also like to thank my close friends Bhargavi, Anusha, Ram, Yashi, Priyanka, Rakesh, Inder, Sandeep, Raj, and Bhavani, who have been like a family away from home. Thank you all for your constant love and support through thick and thin.

TABLE OF CONTENTS

Chapter	Page
1. INTRODUCTION	1
1.1 Discharges in electrical insulation.....	1
1.2 Significance of PD in electrical insulation.....	2
1.3 Physics of Discharge processes	4
1.4 Need for PD detection and analysis	8
1.5 PD detection techniques	9
1.6 Analysis of PD data.....	14
1.7 Objective of the thesis and documentation outline	20
 2. ANALYSIS OF PD PULSE HEIGHT PARAMETERS	 21
2.1 Introduction	21
2.2 PD data generation	21
2.3 Analysis of PD data.....	24
2.4 Prediction of PD pulse height parameters	31
2.5 Summary	38
 3. EXPERIMENTAL SETUP.....	 39
3.1 Motivation	39
3.2 A Basic straight detection system	39
3.3 Experimental setup description	41
3.4 Description of system components.....	43
 4. RESULTS AND DISCUSSIONS.....	 52
4.1 Prediction of parameters using linear prediction method.....	52
4.2 Prediction of parameters using artificial neural networks.....	57
4.3 Comparison of the two techniques	62

Chapter	Page
5. CONCLUSION AND FUTURE WORK.....	65
REFERENCES.....	67
VITA.....	70

LIST OF TABLES

Table	Page
4.1 Comparison of means square errors of both methods.....	65

LIST OF FIGURES

Figure	Page
1.1 Void inclusion between two electrodes.....	5
1.2 Equivalent circuit of dielectric with a void.....	6
1.3 Schematic of a straight detection circuit.....	9
1.4 Straight detection circuit.....	10
1.5 Balanced detection circuit.....	12
1.6 Parameters of a PD pulse.....	14
1.7 Pulse sequence parameter.....	19
2.1 The setup used for measuring PD.....	22
2.2 Block diagram of various steps followed in a typical aging sequence.....	23
2.3 Regions in (β_1, β_2) plane for various distributions.....	26
2.4 Shape parameters for samples A and B.....	28
2.5 Scale parameters for samples A and B.....	29
2.6 Performance for shape parameter of sample B using linear prediction.....	33
2.7 A simple neuron.....	34
2.8 An interconnection of neurons to form a neural network.....	35
2.9 An Elman neural network.....	36
2.10 Performance for shape parameter of sample B.....	37
3.1 A basic experimental setup.....	39

Figure	Page
3.2 Schematic of the experimental setup.....	41
3.3 Schematic diagram (including layout) of the setup.....	42
3.4 Outside of the EM Test Chamber.....	43
3.5 Discharge free transformer.....	44
3.6 Power Separation Filter.....	45
3.7 Charge Injection Capacitor.....	46
3.8 Test Cell.....	47
3.9 Complete view of the control chamber of PD measurement setup.....	48
3.10 The control panel of the DDX-7000 Discharge Detector.....	49
3.11 A shot of the front panel of the DDX detector.....	50
3.12 PD measurement system from Italian company TECHIMP.....	51
4.1 Prediction performance for shape parameter of sample A.....	55
4.2 Prediction performance for shape parameter of sample B.....	56
4.3 Prediction performance for scale parameter of sample A.....	57
4.4 Prediction performance for scale parameter of sample B.....	58
4.5 Prediction performance with 10 neurons.....	60
4.6 Prediction performance with 30 neurons for shape parameter.....	61
4.7 Prediction performance with 30 neurons for scale parameter.....	62
4.8 Prediction performance with 22 neurons.....	63
4.9 Prediction performance with 24 neurons.....	64

CHAPTER 1

INTRODUCTION

This chapter gives an introduction to the basic concepts and terminology that form the foundation of this thesis and also provides a brief review of the work done in the general area of this research.

1.1 Discharges in Electrical Insulation

Electrical insulation plays a significant role in any high voltage power setup. An *electrical discharge* results from the creation of a conducting path between two points of varied electrical potential in the medium in which the points are immersed. A *Partial Discharge* or *PD* is an electrical discharge that only partially bridges the insulation between these conductors.

Krueger points out that PD can be broadly distinguished into three types for diagnostic purposes: *internal discharges*, *surface discharges* and *corona* (Ref [1]). They are fittingly defined by Mason in Ref [2] as:

(a) *Internal discharges* “are caused by gaseous inclusions, or particles, *e.g.* metal, or glass and cellulose fibers, in solid, liquid, or impregnated insulation. Gaseous inclusions may arise during manufacture, or develop during approval tests, or in service, as a consequence of mechanical stresses, thermal cycling, overload, or overvoltage conditions.”

(b) *Surface discharges* “occur in gases, or liquids, from the edges of conductors, on to the surface of insulation, where it is not covered by the conductor and are remote from solid insulation.”

(c) *Corona* “occurs in gases, around conductors” Ref [2].

The three types of PD give rise to different characteristics and also affect the life of insulation differently. At normal operating stresses, internal and surface discharges cause progressive degradation of insulation and its eventual breakdown. At higher stress they may cause breakdown soon after application of voltage. Surface discharges may also be caused by moisture and ionic contamination of the insulating material, which can lead to breakdown. Corona in air generates ozone, which can cause stress leading to cracking of insulating material and release of nitrogen oxides that along with water vapor, may corrode metals and form conducting deposits on insulation leading to an eventual breakdown.

1.2 Significance of PD in electrical insulation

The electrical insulation of equipment like motors, transformers, and generators is prone to various chemical attacks, thermal stresses, and abrasions due to movements. In all these cases, these stresses will weaken the bonding properties of the epoxy or polyester resins that coat the insulation. These are explained in detail by Koing in Ref [3]. As a result of these various stresses, air pockets or ‘voids’ will develop within the insulation.

As the gas within the void has a dielectric constant, that is much less than its surrounding material, it experiences a considerably higher electric field. When this becomes high enough to cause electrical breakdown in the gas, a partial discharge occurs. PD can also occur along the surface of solid insulating materials if the surface electric field tangential to its surface is high enough to cause a breakdown along the insulator surface. This phenomenon commonly manifests itself on overhead line insulators, particularly on contaminated insulators during days of high humidity as explained in detail in Ref [4].

The effects of PD within high voltage cables and electrical equipment can be very severe, ultimately leading to complete failure. The collective effect of partial discharges within solid dielectrics leads to the formation of numerous conducting discharge channels branching partially. This process is called ‘treeing’ Ref [5]. Repetitive discharge events cause irreversible mechanical and chemical deterioration of the insulating material. Damage is caused by the energy dissipated by high energy electrons or ions, ultraviolet light from the discharges, ozone attacking the void walls, and cracking as the chemical breakdown processes release gases at high pressure (Ref [6, 7]). The chemical transformation of the dielectric also tends to increase the electrical conductivity of the dielectric material surrounding the voids. This increases the electrical stress in the unaffected gap region, accelerating the breakdown process. In paper-insulated high-voltage cables (Ref [8]), partial discharges begin as small pinholes penetrating the paper windings that are adjacent to the electrical conductor or outer sheath. As PD activity progresses, the repetitive discharges eventually cause permanent chemical changes within

the affected paper layers. Over time, partially conducting carbonized trees are formed. This places greater stress on the remaining insulation, leading to further growth of the damaged region, resistive heating along the tree, and further charring (sometimes called *tracking*). This eventually culminates in the complete dielectric failure of the cable and, typically, an electrical explosion.

PD dissipates energy in the form of heat and sometimes as sound and light like the hissing and dim glowing that can be observed from the overhead line insulators or transformers. Heat energy dissipation may cause thermal degradation of the insulation. For high voltage equipment, the health of the insulation can be confirmed by monitoring the PD activities that occur through the equipment's life. To ensure reliability and long-term sustainability, PD in high-voltage electrical equipment should be monitored closely with early warning signals for inspection and maintenance as mentioned in Ref [1] and also in Ref [10].

Hence, occurrence of PD is harmful to the health of any electrical instrument; therefore, it is necessary to study the physics of partial discharge processes to help analyze this phenomenon better.

1.3 Physics of Discharge processes

Every material has an electrical breakdown (dielectric) strength that represents the electrical intensity necessary for current to flow and an electrical discharge to take place. Common insulating materials such as epoxy, polyester, and polyethylene have very high dielectric strengths. Conversely, air has a relatively low dielectric strength. Electrical

breakdown in air causes an extremely brief (lasting only fractions of a nanosecond) electric current to flow through the air pocket. The measurement of partial discharge is in fact the measurement of these breakdown currents. This was studied by Bartnikas and is explained in detail in Ref [10]. The rest of the matter in this section has been mostly studied and stated from this reference.

The most common cause for breakdown in electrical insulation systems is from void inclusions. Electrical breakdown can occur in a gaseous, liquid or solid insulating medium. It is often initiated within gas voids enclosed in solid insulation, in bubbles within a liquid insulating material such as voids in an epoxy insulator, or in gas bubbles dissolved within transformer oil.

Voids are generally formed during one of the various steps involved in the process of manufacture of insulation materials. For example, voids are created in polyethylene cables during the extrusion process. Voids concealed in the insulation system of electrical equipment or apparatus are always subjected to higher electrical stress than their adjacent insulation media (solid or liquid).

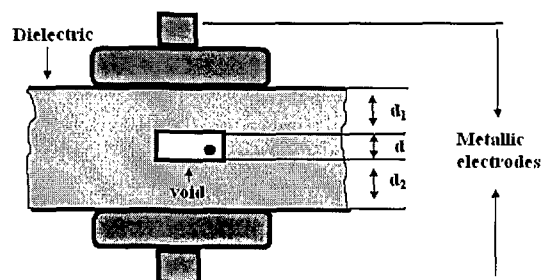


Fig.1.1: Void inclusion between two electrodes.

Consider a simple void that is in series with a solid or liquid insulation as shown in the Figure 1.2. Let it be subjected to an average electrical stress ' E ' with a dielectric constant ' ϵ ' and the void is enclosed by two dielectric layers with thickness d_1 and d_2 with the same dielectric constant ' ϵ_0 '. If E_d is the voltage drop across the layers and E_b is the breakdown voltage of the void, then the void will break down or commence to discharge at a peak value of applied voltage E given by

$$E = \frac{E_b}{d} \left(\frac{d_1 + d_2}{\epsilon_0} + 1 \right) \quad (1-1)$$

Where $E = E_b + E_d$

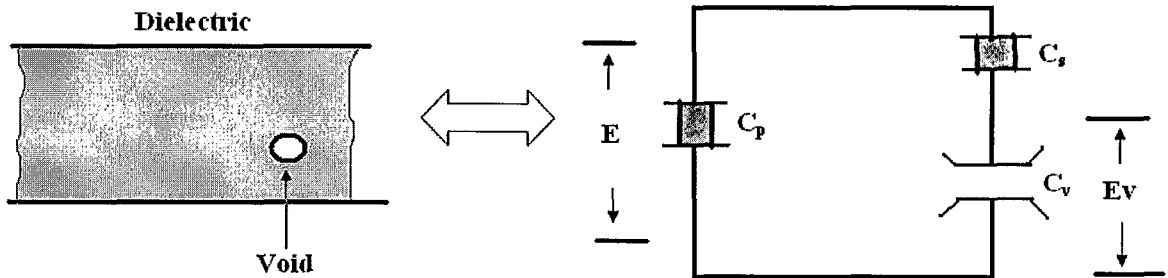


Fig.1.2: Equivalent circuit of dielectric and void.

The parameters associated with partial discharge can be obtained by representing the discharge process in voids by its equivalent circuit (figure), as proposed by Austen and Hackett in Ref [2]. In the circuit, C_v represents the capacitance of the void, C_s is the total capacitance in series with the void and C_p is the remaining capacitance of the dielectric shunting the series combination of C_v and C_s . When a discharge takes place in

the void, the voltage drops across C_v by a value ΔE from its initial value E_b . To restore this voltage drop, the charge across capacitance C_p must be

$$\Delta Q = \frac{\Delta E C_s C_v}{C_s + C_v} \quad (1-2)$$

Under normal conditions this reduces to $\Delta Q \approx \Delta E \cdot C_s$, which represents the charge transfer in the void at the instant of discharge.

Hence the energy dissipated in each discharge is given by

$$\Delta W = C_v \cdot \Delta E \left(E_b - \frac{\Delta E}{2} \right) \quad (1-3)$$

And in the case where E_b corresponds to instantaneous sinusoidal voltage value across the void at the breakdown instant, the energy expression simplifies to

$$\Delta W = \frac{1}{2} C_v [\Delta E]^2 \quad (1-4)$$

This discharge energy given by ΔW is an important quantity since the degradation rate of insulating material exposed to discharges is directly proportional to the energy released by the discharges.

1.4 Need for PD detection and analysis

It is established in the previous sections that the occurrence of PD in dielectric material degrade and erode it, leading to the breakdown of the electrical equipment. PD detection is important to ensure that the equipment is healthy and in operational condition. PD detection can be used to monitor the condition of the installation of the

equipment and in the quality assessment of the insulation. PD measurements are studied to explain the partial discharge phenomena and to assess the quality of the electrical equipment.

By means of partial discharge analysis, unexpected in-service failures of the equipment can be avoided, age of the equipment can be predicted, the quality of maintenance repairs, can be assessed, and improve the overall reliability of the system can be assessed. Due to PD measurements and their analysis, vital information is gathered regarding several aspects of insulation aging, which is useful in the case of verification of equipment integrity and diagnosis. Hence detection of PD, their measurement, and analysis of the PD data obtained is vital in the study of electric breakdown and partial discharge. The following sections introduce the basic techniques and concepts of PD detection, measurement and analysis.

1.5 PD detection techniques

PD detection is the first and a very crucial step in analyzing the partial discharge phenomenon. There are two important PD detection techniques discussed in Ref [1, 10] that form the basis of most of the latest PD detection equipment. They are:

- Straight detection method
- Balanced detection method.

1.5.1 Straight detection

Figure 1.3 shows the block diagram of a straight-detection circuit obtained from Ref [10].

It contains a voltage source in series with a capacitive coupling and pulse detection

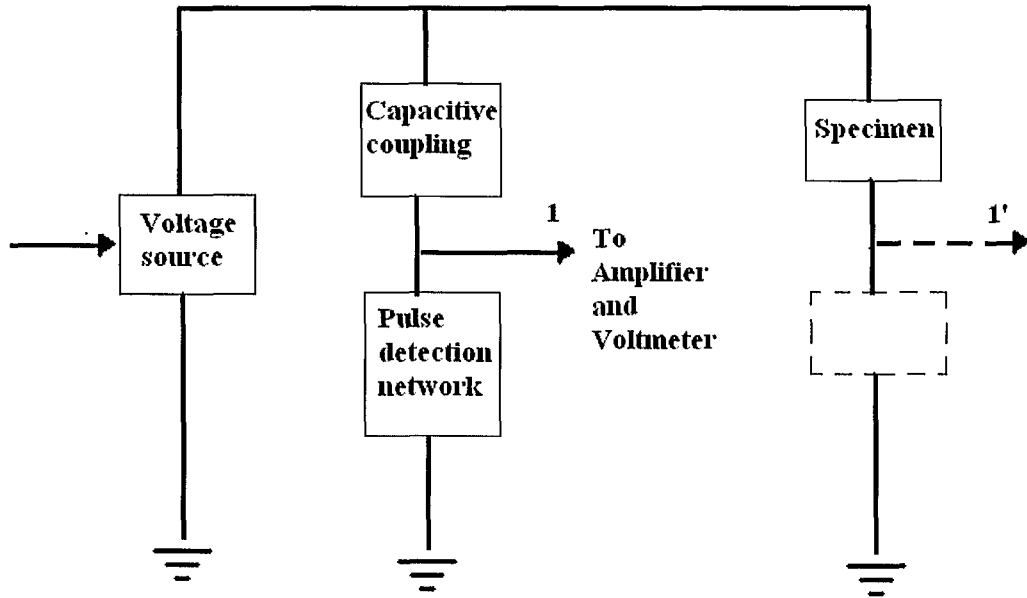


Fig.1.3: A typical straight detection circuit.

network across which the PD are to be detected for a given specimen. The specimen to be tested can be connected in two ways, with the alternate way being represented by dotted lines. The second connection is the one in which the pulse-detection network is in series with the specimen that can be isolated from the ground. This connection is useful when the coupling capacitance is greater than the specimen capacitance; their inverse ratio will decrease the pulses induced or generated in the high-voltage circuit. Two types of pulse-detection circuits are employed in this type of detection- either RC or RLC with RLC being used most commonly.

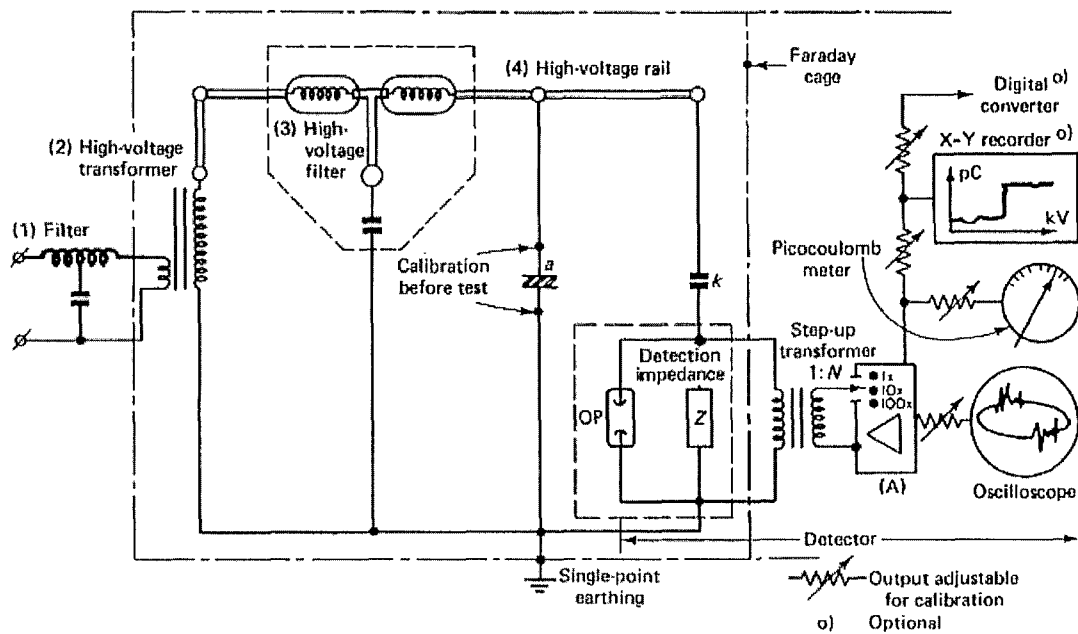


Fig.1.4: Straight detection circuit by Krueger, Ref [1].

A typical straight detection circuit is shown in figure 1.4. The voltage source contains a filter to suppress any sort of interference. The discharge-free high voltage transformer is also connected to a high-voltage filter to suppress further interference and discharges from the transformer. The calibrating capacitor 'C' can be connected in two ways as suggested in the block diagram. Specimen 'a' is usually connected between high voltage and earth. A coupling capacitor 'k' must be discharge free. The detection impedance 'Z' is usually shunted by an over voltage protection. The output from the pulse detection circuit is given to a step-up transformer (1:N) which is connected to an amplifier with a bandwidth wider than that of the impedance at which the discharges are to be measured. Amplifier 'A' has a bandwidth higher than that of the detection

impedance to successfully amplify the PD obtained. An X-Y recorder is connected to the amplifier output to view the PD in the desired scale and quantity.

The performance of straight detection can be characterized by these quantities:

(1) The shape and size of impulse detected at the impedance give the response to a discharge 'q'. The height of the response is given by:

$$v = \frac{q}{a+(1+n)C} \quad \text{Where } n = a/k. \quad (1-5)$$

(2) The sensitivity (smallest detectable charge) is given by

$$q_{sen} = 4 \cdot 10^{-4} \cdot \frac{\sqrt{n+1}}{\zeta} \cdot \sqrt{a + (1 + n)C} \quad (1-6)$$

where ζ is the response of the amplifier.

(3) System calibration is generally achieved by insertion of a square wave produced by a pulse generator into the system at a location related to the terminals of the specimen. The rise time of the calibrating pulse should correspond to a frequency higher than the operational frequency of the overall discharge detector.

The straight detection technique is the most basic technique that can be used to detect PD of any specimen. If more than one specimen is to be tested, the balanced detection technique can be used.

1.5.2 Balanced detection

Figure 1.5 is the setup of a typical balanced or bridge detection circuit.

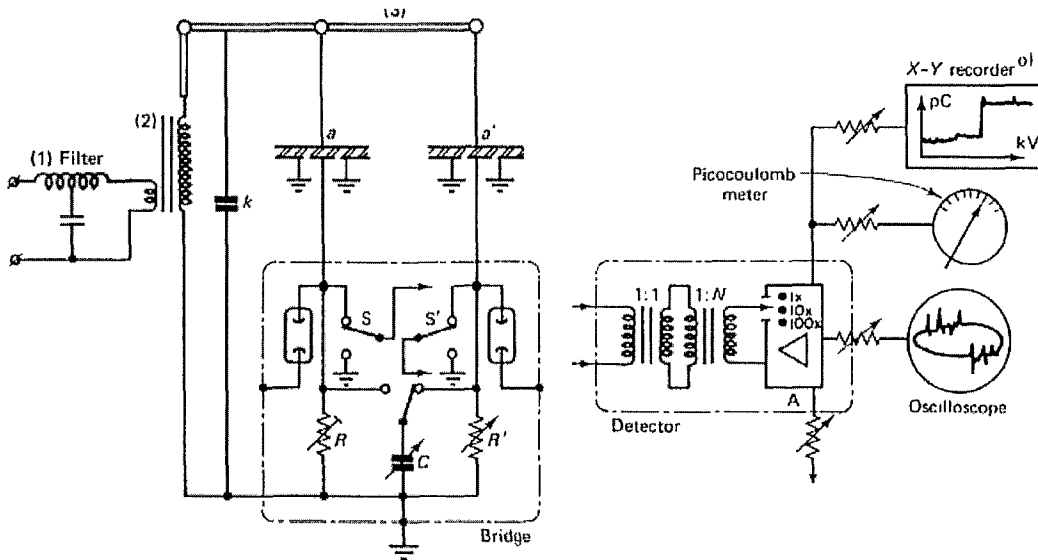


Fig.1.5: Balanced detection circuit by Krueger, Ref [1].

The construction is pretty similar to the straight detection circuit but here filtering can be less severe and, the high voltage transformer may show some discharges. The coupling capacitor is not needed here. In figure 1.5, two specimens a and a' are shown, but a single specimen can be balanced against a paper insulated coupling capacitor or a compressed gas standard capacitor. The pulse circuit contains two resistors R and R' , capacitor C and switches S and S' as shown above. R is switchable in a limited number of steps to match the sample capacity and keep the time constant $R \times C$ a constant. R' is variable and can be fine-tuned to achieve balance in the bridge. If switch S is switched, discharges in the specimen disappear, discharges in a' remain and external discharges increase. This is the main difference between straight and balanced detectors. Straight detection cannot identify relevant and external discharges separately, while balanced

detectors can do so using this switch. The signals from the pulse circuit are fed to a bridge transformer which has a 1:1 ratio to maintain symmetry.

The performance of straight detection can be characterized by these quantities:

- (1) The size and shape of pulses fed from bridge points are given by

$$v = \frac{q}{a+C+(1+n)C'} \quad (1-7)$$

- (2) The sensitivity (smallest detectable charge) is given by

$$q_{sen} = 4 \cdot 10^{-4} \cdot \frac{\sqrt{n+1}}{\zeta} \cdot \sqrt{a + C + (1 + n)C'} \quad (1-8)$$

- (3) In terms of calibration, internal calibration is less risky in bridge detection as compared to balance detection because the calibrated pulse is injected in the series connection of the two specimens.

1.6 Analysis of PD data

The next step after detecting and measuring PD data is its analysis. The first step in analyzing PD data is to find the parameters that can be directly determined or calculated from the raw data measured. Figure 1.6 shows a typical PD pulse and the parameters associated with it. Here, the PD of a specimen are measured with reference to one power line cycle (PLC), which is typically a sine wave of known frequency.

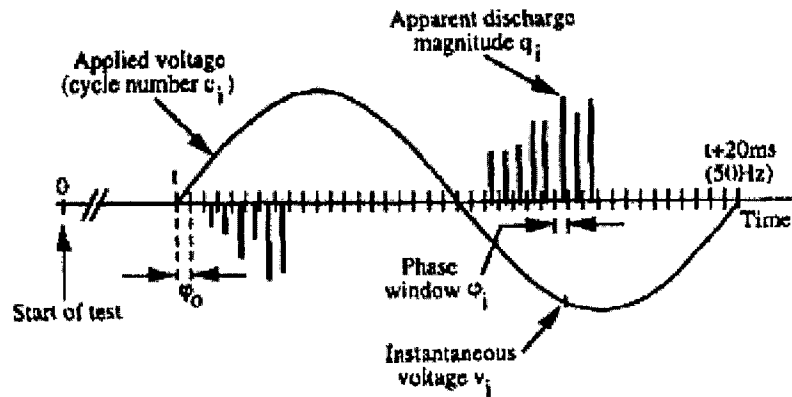


Fig.1.6: Parameters of a PD pulse by Kuffel and Zaengl, Ref [11].

The parameters are:

- Instantaneous applied voltage v_i (volts);
- Apparent magnitude of discharge q_i (coulombs);
- Time of occurrence t_i (seconds) relative to the beginning;
- Relative Phase position ϕ_i (degrees);
- Total number of discharges recorded n ;
- Discharge energy w_i (joules);
- discharge polarity p_i (positive or negative);
- Total time interval of measure ' T ' (seconds);

Based on these parameters the analysis of PD data can be categorized into three techniques; each analysis involves a different way of using these parameters for successful interpretation, evaluation or prediction of PD data. These analysis techniques are:

- (a) Pulse Height Analysis,
- (b) Pulse Phase Analysis,
- (c) Pulse Sequence Analysis.

1.6.1 Pulse Height Analysis

(i) *Apparent charge (q)* is defined in Ref [12] as the “the change in charge that, if injected between the terminals of the device under test, would change the voltage across the terminals by an amount equivalent to the PD event.”

Apparent charges are measured in PD data because actual charge change occurring while detecting PD in a specimen is not measurable. The apparent charges usually expressed in picoCoulombs (pC) and can be obtained by the equation

$$q = C_b \Delta(V_c) \quad (1-9)$$

where C_b = break-down capacitance

$\Delta(V_c)$ = voltage difference across the specimen at that instant

The integrated quantities that can be measured using apparent charge are defined by the IEC 270 standards as:

Average discharge current (A):

$$I = \frac{1}{T} (\sum_{i=1}^n mod(q_i)) \quad (1-10)$$

Discharge power (W) :

$$P = \frac{1}{T} (\sum_{i=1}^n q_i v_i) \quad (1-11)$$

Peak discharge magnitude (C):

$$q_{\max} = \max (q_1, q_2, \dots, q_n) \quad (1-12)$$

Average discharge magnitude (C):

$$q_{ave} = \frac{1}{n} (\sum_{i=1}^n mod(q_i)) \quad (1-13)$$

As evident from the above equations, q is directly related to the discharge energy, the size of the defect and can be easily measured with any electrical discharge detector (Ref [1]). Hence, apparent charge has evolved as an attractive parameter to analyze discharges.

(ii) *Pulse Height Distribution Parameters*: The PD pulses are classified into different class intervals based on their magnitudes. The different classifications are studied as a histogram to understand their distributions; four moments of this histogram are mean (M_1), variance (M_2), skewness (M_3) and kurtosis (M_4). The two parameters that can identify the pulse height distribution (say β_1 and β_2) can be derived by the above 4 moments using the karl-perason's formula as in Ref [13]. Based on the values of β_1 and β_2 , the type of distribution can be determined.

Once the type of distribution is determined, maximum likelihood estimate or any graphical technique can be used to determine the parameters of distribution. Generally,

these parameters provide information on the magnitude, the spread and the shape of the distribution.

1.6.2 Pulse Phase Analysis

This technique makes use of the instantaneous phase ' φ_i ' values for analysis of PD data. In this technique, the obtained phase angle is divided into a number of small windows.

An analysis algorithm is written that calculates the integrated parameters over that period for each phase window and plots it as a function of the phase position ' φ '. Some of the most common plots obtained which are used in Ref [14, 15, 16, and 17]:

(φ, n) : 2 D plot of phase and number of PD in each window;

(φ, i) : 2 D plot of phase and average discharge current in each window;

(φ, q_{ave}) : 2 D plot of phase and average discharge magnitude in each window;

(φ, q_p) : 2 D plot of phase and peak discharge magnitude in each window.

Different types of insulation defects produce different discharge patterns. If these differences can be included in a knowledge base, inference of the defect type from the observed PD pattern may be possible (i.e. an expert system). An important characteristic that is difficult to quantify is the variation of some patterns with time. Allowance must be made for this in any monitoring system.

Apart from these uni-variate distributions, a bi-variate distribution such as $n(\varphi, q)$ can be generated. It can be described as a “two-dimensional array where, in addition to the phase position φ_i , the range of discharge magnitude is also quantized into a finite number of intervals q_j . The value of an entry n_{ij} in this array represents the number of PD pulses having magnitude q_j and phase position φ_i . The array is normalized with respect to the integration period so that its entries become the pulse repetition rate, i.e. number of pulses per second. The visualization of such a distribution requires a three -dimensional (3D) plot” Ref [18]. This 3D plot of $n(\varphi, q)$ is very important in analyzing and determining a specimen’s lifetime. A lot of work has been done in this area as presented in Ref [11, 17, and 19].

1.6.3 Pulse Sequence Analysis

This technique, a relatively new approach to PD analysis, was introduced only a decade ago in Ref [12]. It is based on considering the measured pulses as a sequence and using sequence properties to identify parameters and characteristics of PD that can be measured easily.

The basic methodology of this technique is well described in Ref [20] as “the pulse sequence data obtained from a PD record can be viewed as a train of pulses with varying magnitude and time intervals accumulated over a number of alternating cycles.”

In this technique, depending on the structural properties of a sequence, PD pulses are processed. Based on the time interval between pulses the PD sequence is basically

grouped as a ‘cluster.’ A cluster is typically characterized by its structural parameters as shown in the figure below:

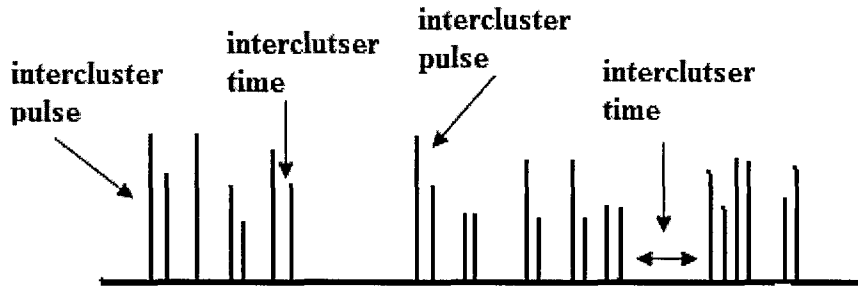


Fig.1.7: Pulse sequence parameters.

The definition of terms used in the representation are as follows, obtained from Ref [21]:

- Inter-cluster charge magnitude : charge magnitude of the first pulse in a cluster;
- Inter-cluster time : time between two clusters;
- Intra-cluster charge magnitude: charge magnitude of pulses within a cluster, except for the first pulse;
- Intra-cluster time : time between pulses within a cluster;
- Cluster size: number of pulses in a cluster.

The characteristics of this cluster can depict the PD breakdown mechanism very efficiently. This analysis technique is especially used for PD at a low electric field and when there are only few discharges per cycle of the applied voltage. By using Pulse

Sequence Analysis, the obtaining sequence patterns for two separate charges at one point are characteristically different (Ref [22]).

1.7 Objective of the thesis and documentation outline

From the previous sections of this chapter it can be stated with the aid of the studied literature that the stage of insulation breakdown can be identified by the parameters of PD distribution. Hence prediction of these parameters can be useful in identifying the possibility of future failure in insulation. The main objective of this thesis is to introduce two new techniques to predict the partial discharge pulse-height parameters. The two techniques will be developed using linear prediction and artificial neural networks respectively.

This thesis is organized as follows:

Chapter 2 documents the main contribution of this thesis. It explains the analysis of partial discharge data and presents the two techniques developed for the prediction of PD pulse height distribution parameters.

Chapter 3 describes the schematic diagram and components of an experimental setup that will be used for further research work on the thesis topic.

Chapter 4 shows the results obtained from the simulation of the two prediction techniques.

Chapter 5 summarizes the conclusions made from the work done and discusses the work to be done in the future to further advance the research on this topic.

CHAPTER 2

ANALYSIS OF PD PULSE HEIGHT PARAMETERS

2.1 Introduction

Analysis of partial discharge data is intrinsically complex. The PD height data has to be quantified such that its parameters represent their magnitude and the shape of the distribution. The quantification procedure used in this thesis is based on an earlier work that uses statistical analyses (Ref [23]) and digital signal processing techniques (Ref [24]). The next step of analysis after obtaining the parameters is their prediction. In this work, two techniques, namely linear prediction (Ref [25]) and artificial neural networks (Ref [26]), are used to predict these PD parameters. The details of these two prediction techniques are described in this chapter. The prediction is performed on a set of PD data that was generated from two different samples made of polymethyl methacrylate (PMMA) material. The process of data generation and its analysis to obtain the pulse-height parameters has also been explained in detail here. The simulation results of the two prediction techniques are presented in chapter 4.

2.2 PD Data generation

The experimental setup that was used for obtaining PD data is shown the Figure 2.1 (Ref [23]). The experimental results were obtained by Dr. P. Basappa in an earlier

investigation. These results were used to test analysis techniques developed during the present research.

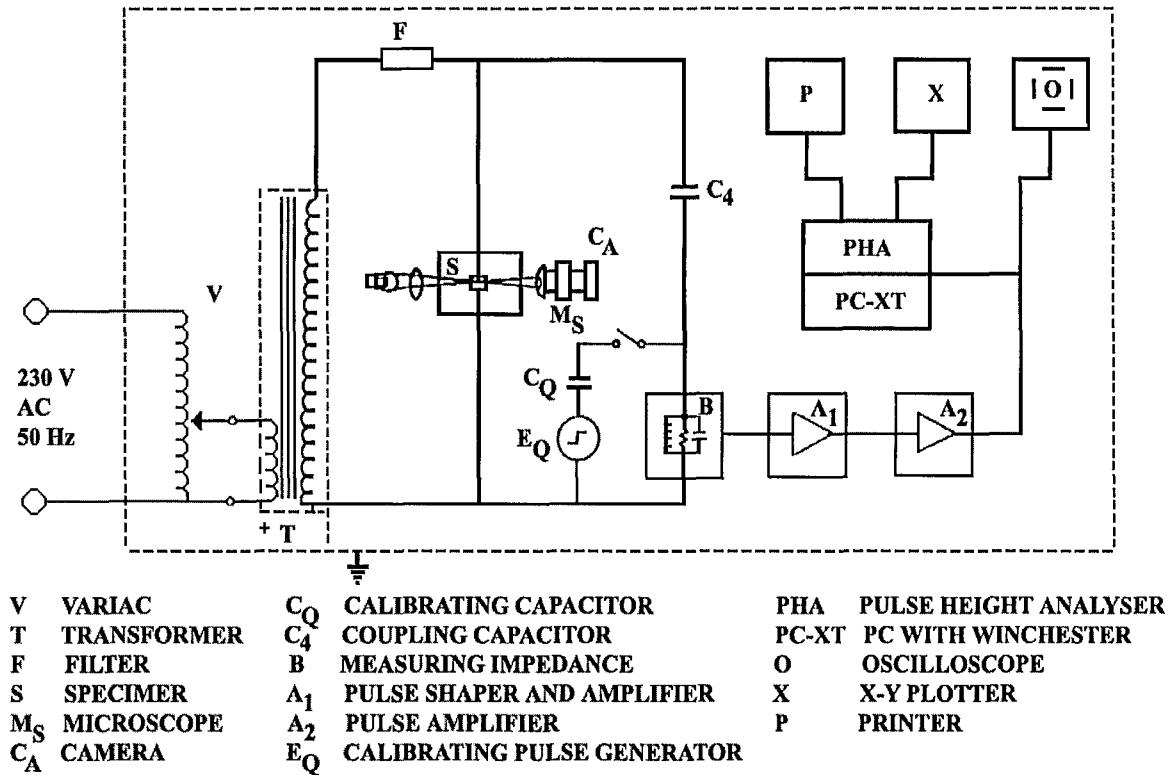


Fig. 2.1: The set-up used for measuring PD (by Basappa et al. Ref [23]).

A brief description of the experimental setup is taken from Ref [23], reprinted with permission from author. The AC voltage was applied through a 230V/50 KV, 5 KVA, 50 Hz (General Electric) transformer, the primary voltage being controlled by an auto transformer. The filter “F” inhibited the transfer of high frequency pulses to the measuring circuits. The specimen (PMMA) was kept in an oil cell to prevent surface discharges. A coupling capacitor C₄ (4400pf) was connected to both the specimen and the transformer as shown in the figure2.1. The other end of the capacitor C₄ was connected to

the LRC measuring impedance tuned to 500 KHz. The pulses across this impedance were amplified using two amplifiers, A_1 and A_2 , where A_1 is a tuned amplifier that shapes and pre-amplifies the pulse and A_2 is a pulse amplifier that controls the attenuation and gain so that the magnitude of the pulses fall within the measurable range of the multi channel analyzer. The trees were photographed periodically using a micro photographing system (MS) without interrupting the voltage applied to the specimen. The pulse height analyzer (PHA) resident in the data acquisition computer was where records of pulse magnitude spectra were collected. Breaking the amplitude spectra into class intervals, fitting distributions to them, checking the degree of fit (graphically and by chi-squared test) were all accomplished using a computer.

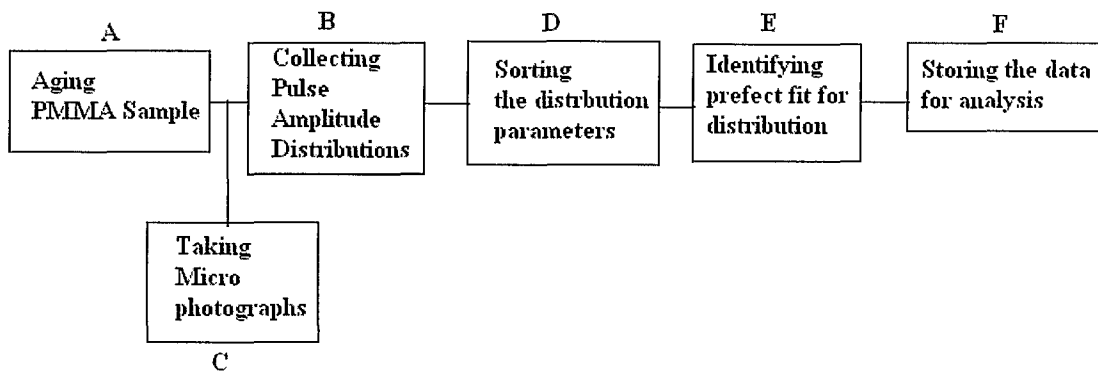


Fig 2.2: Block diagram of various steps followed in a typical aging sequence (Ref [23]).

The sequence of events that occur from aging a sample to analyzing the data obtained is shown in Figure 2.2. The PD aging process was monitored by two methods. The first was the collection of partial discharge amplitude distributions for a pre-determined duration of 5 minutes each and at regular intervals of 5 minutes (block B). The other was

taking the photographs of the tree periodically without interrupting the voltage applied to the specimen (block C). The PDs were continuously observed on the oscilloscope so that the attenuation and gain adjustments could be done to contain the range of PDs within the measurable limits of the pulse height analyzer (PHA). The pulse height amplitude spectra were stored as sequentially numbered files up to the end of the aging process. The PD pulse counts were sorted into different class intervals using earlier noted attenuation and gain factors (block D). These results were fitted with statistical distributions, and the degree of fit was checked for all the sequential files (block F).

2.3 Analysis of PD data

Based on the process given above, several PMMA samples with embedded needles were aged. The growth of the tree was monitored by taking photographs of the tree and by measuring the partial discharge with the pulse height analyzer (PHA). The pulse amplitude distribution was obtained. The lowest pulse magnitude was observed to be generally at least twice the noise magnitude; thus, the data presented was considered to be truncated at about twice the noise level (2 pC).

As the aging progressed, pulse magnitude distribution was accumulated for every 5 minutes. After each 5 minute interval the counts in all the channels were set back to zero. This was repeated at intervals of 5 minutes. Frequency distribution curves were fitted to the data, and the parameters of the distribution were estimated. The total number of pulses was usually greater than 25,000. The obtained PD pulses were acquired by the pulse height analyzer and sorted into different class intervals based on their attenuation

and gain factors. For these pulse amplitude distributions, the first four moments of distribution (mean, variance, skewness and kurtosis) were calculated and the sample estimates ' β_1 ' and ' β_2 ' were calculated. The sample data was then subjected to the standard statistical tests discussed below:

(a) The Trend Test: This detects a monotonic trend, if any, in a sequence of observations. The trend test is more powerful than a run test. However, the test however fails if there is fluctuating trend in the given sequence.

(b) Distribution Identification Test: A distribution is completely defined once all its moments are known, however many distributions can be adequately described by the first four moments. In Ref [27] Pearson has developed a method for identifying the distributions with the help of β_1 and β_2 , which are functions of first four moments.

The K^{th} moment μ_k about the expected value or central moment is defined as

$$\mu_k = \frac{1}{n} \sum_{i=1}^n (a_i - \mu)^k \quad (2-1)$$

where

n = number of observations

a_i = the i^{th} observation

μ = Arithmetic mean.

Two factors, the skewness and the kurtosis, define the shape of a distribution function.

The degree of skewness indicates the lack of symmetry about the central value and is measured by a factor $\sqrt{\beta_1}$ where

$$\sqrt{\beta_1} = \frac{\mu_3}{(\mu_2)^{\frac{3}{2}}} \quad (2-2)$$

Kurtosis of the curve as compared to the Gaussian distribution can be measured quantitatively by

$$\beta_2 = \frac{\mu_4}{(\mu_2)^2} \quad (2-3)$$

The equations marking the regions of different distributions in β_1, β_2 have been idealized as straight-line equations. As the estimates for β_1 and β_2 of parent population are made from the sample values, and the relations mentioned above are strictly valid for the parent population, the sampling variations have to be taken into account. The regions for various distributions based on the values of β_1 and β_2 are shown in Figure 2.3 obtained from Ref [25]. It should be noted that for an extreme value distribution $\sqrt{\beta_1}$ is negative; and hence $\sqrt{\beta_1}$ was calculated first, and β_1 was calculated from that value. The identification of the distribution was done based on algorithmic conversion of this plot by fixing the lower and upper bounds of β_1 and β_2 .

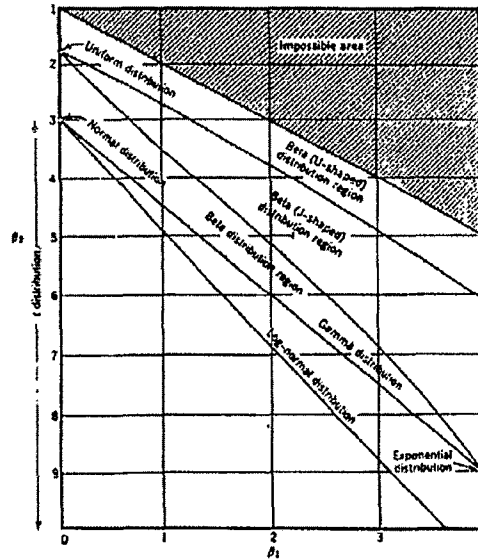


Fig 2.3: Regions in (β_1, β_2) plane for various distributions by Basappa (Ref [23]).

(c) χ^2 Goodness of Fit Test: Once a distribution was identified the estimate of the parameters were made using the appropriate equations obtained from Ref [27]. The goodness of fit of the experimental values with the ideal generated values was measured using the χ^2 goodness of fit test. The values of χ^2 for different degrees of freedom with associated probabilities are available in the form of a standard table.

Based on this analysis, it was found that most of the data could be fitted with weibull, exponential or log-normal distribution, with most of the data modeled in the form of weibull distribution. For the two parameter weibull distribution, the probability density function is given by

$$f(q) = \frac{\eta}{\sigma} \left(\frac{q}{\sigma} \right)^{\eta-1} \left(e^{-\left(\frac{q}{\sigma} \right)^\eta} \right) \quad (2-4)$$

Where q = apparent charge of the PD pulse.

σ = scale parameter of the distribution.

η = shape parameter (slope) of the distribution.

the distribution for the present data can thus be represented as

$$F(q_i) = 1 - \left(e^{-\left(q_i / \sigma_q \right)^\eta} \right) \quad (2-5)$$

Where q_i = the magnitude of the pulse at i^{th} level.

σ_q = the most probable value (63.2 percentile) of q .

η_q = the shape parameter of the distribution.

Assuming the effective capacitance of the system as 'c' and v_q as the voltage amplitude measured as PD, we have from equation (2-5)

$$F(q) = F(c.v_q) = 1 - (e^{-(v_i / \sigma)^\eta}) \quad (2-6)$$

and at the most probable charge magnitude we have $\sigma_q = c.v_q$; $\sigma_v = \sigma$ and $\eta_q = \eta_v = \eta$.

Thus, the distribution may be studied as a PD voltage distribution given by

$$F(v_i) = 1 - (e^{-(v_i / \sigma)^\eta}) \quad (2-7)$$

Based on equation (2-7), the ' σ ' and ' η ' of the PD data collected at regular intervals of time for a complete aging sequence may be considered as a pair of time series of scale parameter (σ) and shape parameter (η). The two time series of scale and shape parameter obtained for the two PMMA samples 'A' and 'B' are shown in Figures 2.4 and 2.5, respectively.

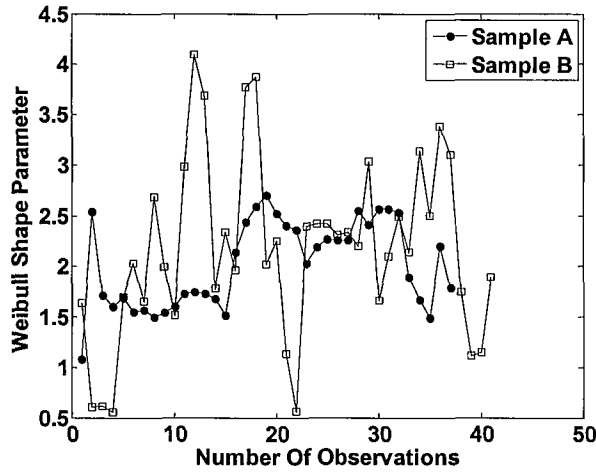


Fig. 2.4: Shape parameters for Samples A and B.

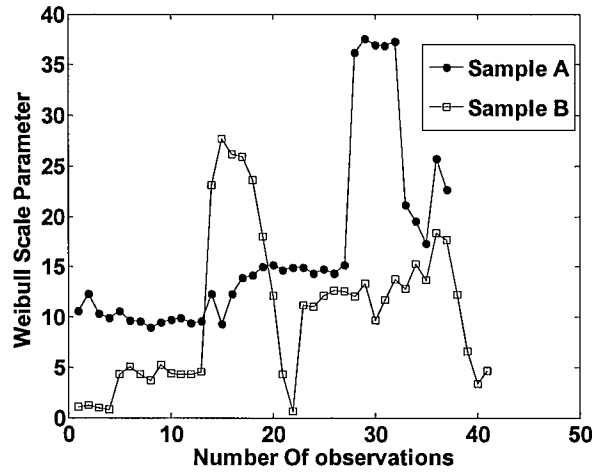


Fig.2.5: Scale parameters for Samples A and B.

After separating the shape and scale parameters, each are analyzed as separate time series using statistical parameters (Ref [26]). For the scale parameter (σ), it is observed that the Time series is composed of a slow varying trend $\sigma_d(t)$ and the fluctuations $\sigma_r(t)$ around the trend so that at any instant 't',

$$\sigma(t) = \sigma_d(t) + \sigma_r(t) \quad (2-8)$$

From the time series, it was observed that the deterministic part $\sigma_d(t)$ can be fitted with a polynomial of the form

$$\sigma_d(t) = a_0 + a_1t + a_2t^2 \quad (2-9)$$

Hence, $\sigma_d(t)$ is the deterministic part, and $\sigma_r(t)$ is the stochastic part at any instant 't' of every ' σ '.

Similarly, for the shape parameter, the time series can be separated into deterministic and stochastic portions, and $\eta(t)$ is represented by

$$\eta(t) = \eta_d(t) + \eta_r(t) \quad (2-10)$$

Where it was observed that its deterministic portion $\eta_d(t)$ is constant with respect to time

$$\eta_d(t) = \frac{1}{N} \sum N \cdot \eta(t_i) \quad (2-11)$$

and N is the number of data points.

2.4 Prediction of PD pulse height parameters

After obtaining the separated deterministic and stochastic portions of the shape and scale parameters of both Sample A and B, the next component of analysis is their prediction. Prediction can be treated as a special case of function approximation when the mapping between the past and future values is to be learned. The predictions for the stochastic variations of the pulse height parameters are achieved through two techniques - Linear Prediction (LP) and Artificial Neural Networks (ANN). The techniques are tested on the PD parameters obtained as explained in the previous section by using MATLAB simulation tools. The theory and working of these techniques are explained in this section.

2.4.1 Prediction of partial discharge pulse heights with Linear Prediction method

Linear prediction (LP) is a method for prediction of values of the experimental data by estimating a linear function based on previous samples of the data. The basic objective of linear prediction is the formation of a linear time invariant (LTI) system. The

behavior of that LTI system is estimated when the inputs and outputs of the system cannot be chosen, i.e. when design of the system is not available.

Based on the observations made on the stochastic portions of the pulse height parameters, it is found that the linear prediction algorithm can be used for their prediction. According to the algorithm, the predicted values can be calculated from the previously obtained output values using the equation:

$$y_p[n] = - \sum_{k=1}^p (b_k y[n - k]) \quad (2-12)$$

Equation (2-8) calculates a set of coefficients that predict the forthcoming output sample $y_p[n]$ based on the knowledge of previous output values $y[n]$, where 'b' is the predictor coefficient. The difference between the actual value of the sample and the predicted value is called the prediction error. This error is ideally a white noise and is given by:

$$e[n] = y[n] - y_p[n] \quad (2-13)$$

Hence, we can rewrite the above equation as:

$$y[n] = e[n] - \sum_{k=1}^p (b_k y[n - k]) \quad (2-14)$$

here the error signal acts as the excitation signal, and predictor coefficients define the model.

To solve this equation, the behavior of the system is observed over some fixed number of samples (N), and set the order is set to ' p ' (that is always less than N). The predictor coefficients are estimated by obtaining values that minimize the energy in error signal over the N samples. We obtain a system of p equations in p unknowns that may be solved to find the best fitting predictor coefficients.

$$\sum_{k=0}^p \left(b_k \sum_{n=0}^{N-1} (y[n-k]) y[n-i] \right) = 0, \quad i = 1, 2, \dots, p \quad (\text{Covariance formulation}). \quad (2-15)$$

$$\sum_{k=0}^p \left(b_k \sum_{n=0}^{N-1} (y[n]) y[n-k+i] \right) = 0, \quad i = 1, 2, \dots, p \quad (\text{Autocorrelation formulation}). \quad (2-16)$$

With these equations, a linear prediction model that can optimally predict future values of the parameters based on a linear combination of past values was obtained. The model was then simulated using MATLAB. When the data set of shape and scale parameters of both sample A and B obtained had M points, the first ' x ' data samples were fed to the model to obtain $x+1$ to M predicted values. The points were trained in the model to calculate the optimal prediction coefficients based on the equations given above. The predicted values were then compared to the corresponding actually obtained values in the set. Prediction error along with the Mean square error of the predicted and actual values was calculated to determine accuracy of the prediction.

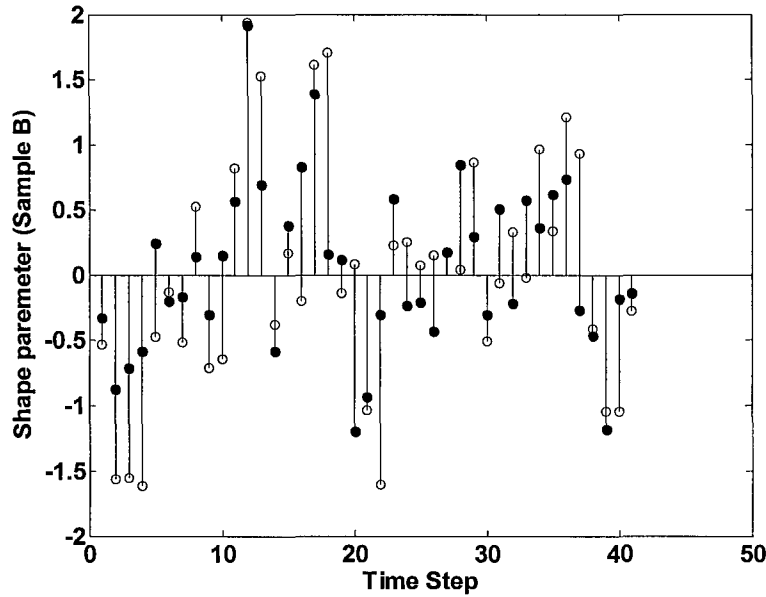


Fig.2.6: Performance for shape parameter of sample B using linear prediction.

Figure 2.6 depicts prediction performance for shape parameter of sample B for the linear prediction model. Filled circles in the figure represent predicted value and unfilled circles show the actual value. Mean square error achieved in the prediction is 0.4095, and prediction error in calculation is 0.3558. For the 37 point data set of sample A, the linear prediction model was able to predict the next 6 values of data with good accuracy.

Since the linear prediction technique is capable of predicting only the stochastic parameters of the PD pulse height parameters, another method that was capable of predicting both the stochastic and deterministic portions of the PD data was required. As both these portions can be represented as a pair of time series, it was observed that artificial neural networks might be useful in their prediction. This technique is presented in the next section of this chapter.

2.4.2 Prediction of Partial Discharge Pulse Heights with ANN:

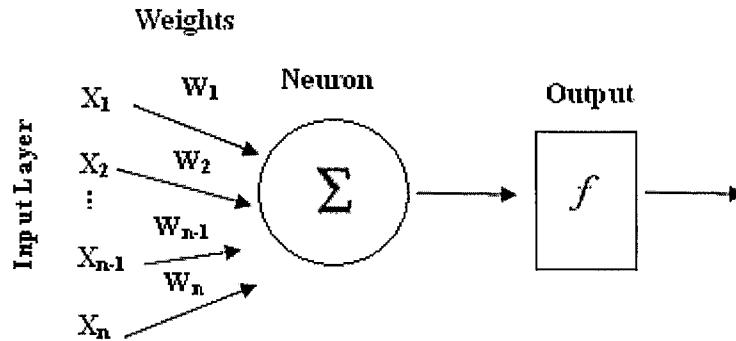


Fig. 2.7: A simple neuron.

A neural network is a biologically inspired, distributed universal function approximation scheme [28]. ANNs are simplified mathematical models of biological neurons and can emulate certain functions of biological neurons such as pattern recognition, pattern identification and associative memory. Certain types of ANNs are capable of learning an arbitrary function ($f: \mathbf{R}^n \rightarrow \mathbf{R}^m$) with a finite number of discontinuities from samples of input and output data with any desired accuracy. Thus, an ANN might be viewed as a black box that takes a column vector of length “n” as the input and produces another column vector of length “m” as the output. A neural network is an interconnection of simple information processing elements called neurons. Figure 2.7 shows a single neuron. The elements of the input vector (X_1, X_2, \dots, X_n) are multiplied by free parameters called weights (W_1, W_2, \dots, W_n) and then summed. The output of the summer is used as an input to a function (that can be nonlinear) to produce the output of a neuron. Figure 2.8 shows an interconnection of neurons to form a neural network. Each circle represents a neuron

similar to the one shown in Figure 2.7. Neurons in an ANN are arranged in layers, and the output of one layer is fed to the input of the second layer. Delayed values of the output of a layer can also be fed back to the input to create neural networks that possess memory and hence can process temporal patterns.

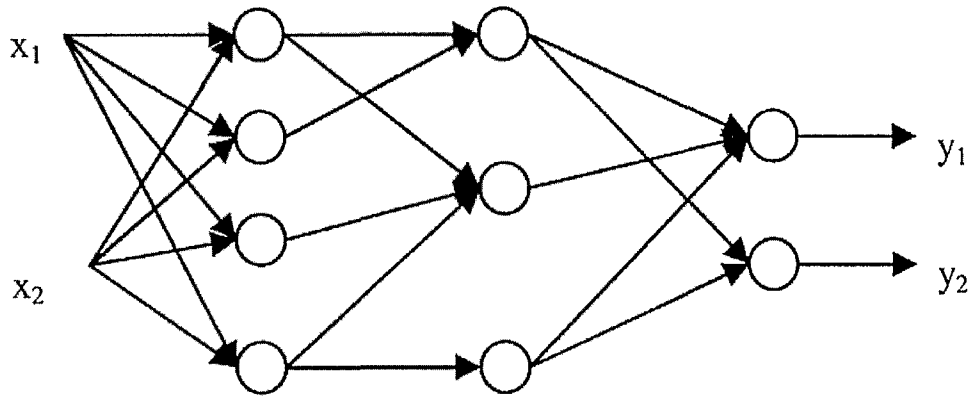


Fig.2.8: An interconnection of neurons to form a neural network.

The ANN is then trained to learn a certain function by adjustment of the free parameters (weights and biases) so as to minimize the mean square error between the actual and desired output vectors. Adjustment of free parameters is achieved by an approximate gradient descent based optimization process. It is known that an ANN with a sigmoidal transfer functions in the first layer and linear transfer functions in the second layer can approximate any function with a finite number of discontinuities.

Since ANNs are capable of learning function, they can also be used for prediction. This is because prediction is a special case of function approximation when the mapping between the past and future values is to be learned. In the case of the partial discharge

prediction problem, future values of the shape and sigma parameter sequences have to be predicted based on previous values. Thus, such networks need memory. This is achieved through the following two approaches:

(a) Providing the current value and delayed values of the sequence as input. In this case the network has finite memory (current prediction depends on a finite number of past values).

(b) Providing a path for the delayed output from the first layer to be fed back to the input. ANNs with feedback connections from the output of a layer to the input are referred to as recurrent ANNs. In this case the current prediction depends on all past values of the input due to feedback (infinite memory).

Recurrent networks are more capable of accurately predicting time series and modeling nonlinear processes. In this technique recurrent ANNs with a sigmoidal first layer and a linear second layer (Elman network) were used.

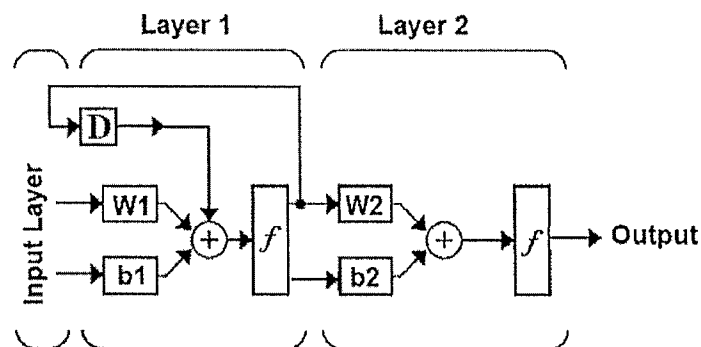


Fig. 2.9: An Elman neural network.

Figure 2.9 shows the recurrent Elman network used to predict scale and shape parameters. The multiplication and summing action of a layer of neurons can be represented using matrix multiplication. $\mathbf{W1}$ and $\mathbf{W2}$ are matrices of weights. $\mathbf{b1}$ and $\mathbf{b2}$ are column vectors of constants called biases. Block \mathbf{D} represents delay elements. The network was then simulated using MATLAB. The prediction performance was observed in a manner similar to the linear prediction, i.e. if the data set of shape and scale parameters of both sample A and B obtained had M points, the first 'x' data samples were fed to train the network to obtain $x+1$ to M predicted values. These predicted values were compared to the corresponding actually obtained values in the set. Mean square error of the predicted and actual values was calculated to determine accuracy of the prediction.

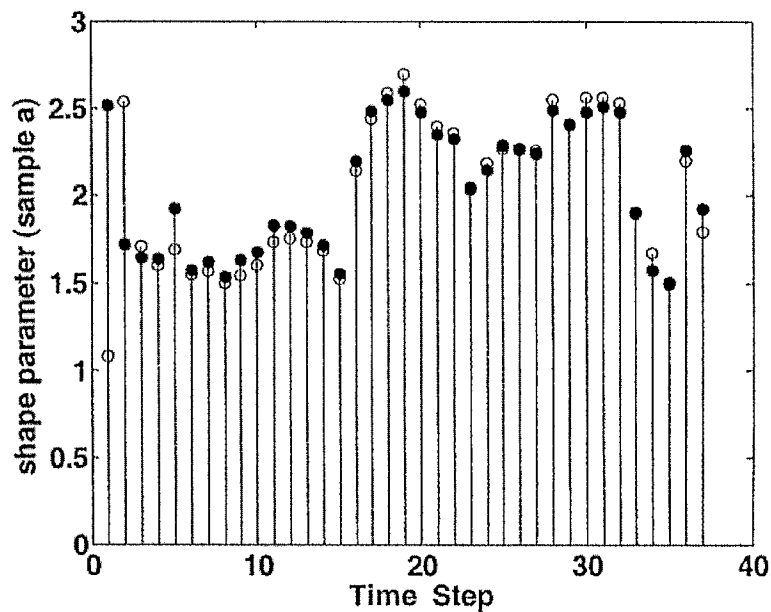


Fig. 2.10: Performance for shape parameter of sample B using artificial neural networks.

Figure 2.10 depicts the prediction performance of the network with 10 neurons for shape parameter of sample A. Filled circles represent the predicted value and unfilled circles show actual value. 30 data points were used for prediction with the total number of data points being 37. Mean square error achieved was 0.0788. For the 37 point data set of sample A, the linear prediction model was able to predict the next 10 values of data with good accuracy.

2.5 Summary

The PD pulse amplitude records obtained at regular intervals of time are quantified by the time-series of shape parameter (η) and scale parameter (σ). The stochastic portions of these time series are used in the process of prediction using linear prediction and artificial neural network techniques. The efficacy of the techniques are evaluated by considering a part of the time series experimental and using the present and past values in this part of the data to forecast the rest of the data. The accuracy of prediction is evaluated through the magnitude of obtained mean square errors (MSE). The performances of all the parameters for both samples using both techniques are presented in chapter 4.

CHAPTER 3

EXPERIMENTAL SETUP

3.1 Motivation

PD in insulation systems are very complex in nature and can only be quantified through probabilistic and statistical means. In addition to the measurement of basic PD quantities, several derived parameters of PD have to be studied for condition assessment of insulation systems. With the advent of fast computers, digitizers and related equipment, new PD parameters can now be effortlessly analyzed. For this purpose, a state of the art PD detection, measurement and analysis system is being developed at the Insulation Evaluation and Design Laboratory (IEDL) at the Marie V. McDemmond center for Applied Research (MVMCAR) at Norfolk State University in Virginia. This facility will be used in further analysis of the work presented in this thesis. This chapter provides a brief description of the schematic and components of this experimental lab setup.

3.2 A basic straight detection system

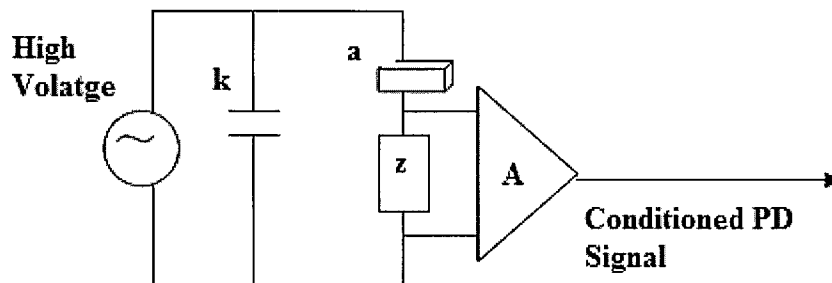


Fig 3.1: A basic experimental set-up.

Figure 3.1 is a basic discharge detection system that provides an understanding of how the experimental setup at IEDL is built. The basic discharge system is built using the straight detection technique and is used to detect PD originating from a test sample 'a' under the influence high voltage. The system consists of a high voltage ac source that should be PD free, a coupling capacitor 'k' connected in parallel with the ac source that facilitates the passage of high frequency current impulses, a detecting impedance 'z' to obtain the output PD pulses and an amplifier 'A' to properly condition these PD pulses. The coupling capacitor 'k' must be of the same order of capacitance as the sample under test 'a' for proper filtering of low frequency impulses. The PD pulses occurring within the sample will cause a high-speed pulse in the detecting impedance 'z', that is then captured for further processing. Typically RC and RLC impedances are used for detecting PD pulses. When sufficient high voltage is applied to this circuit, based on the circuit parameters, the magnitude of the voltage pulse across the detecting impedance will be a function of the magnitude of PD occurring within the sample. The PD pulse's incident across the detecting impedance can then be captured by the discharge detector, which essentially detects and shapes the PD pulse into an acceptable form. Amplifier 'A' provides enough gain for accurate capture of this signal across the detector. Although the commercial detector modifies the original pulse into a standard form, it can only provide us with simple quantities, such as q_{\max} (maximum apparent charge), presence or absence of a PD pulse, background noise level and possibly the most probable part of the power line cycle (PLC) where the PD occurs. Hence, additional equipment such as high speed digitizers and new PD analysis software are required in the experimental setup to obtain additional PD parameters.

3.3 Experimental setup

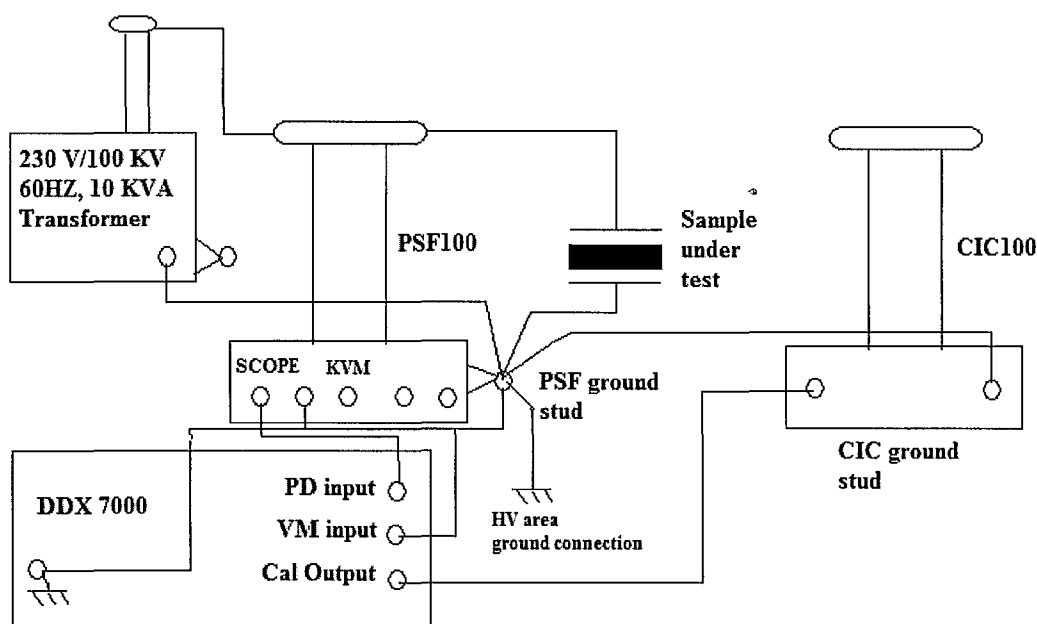


Fig 3.2: Schematic of the experimental setup.

The schematic diagram of the PD detection systems set up at IEDL is shown in Figure 3.2. The 230 V, 60 Hz voltage is fed to the primary of a 100 kV, 10 kVA transformer controlled by a PLC controller. The high voltage output (HV) of the transformer is connected in parallel to a power separation filter (PSF 100), charge injection capacitor (CIC 100) and the test sample as shown in the figure. The ground leads of the apparatus are connected to a single point on the ground to avoid any floating potentials. A quadrapole, which is a part of PSF 100, is connected to the amplifier input, calibration output and KVM input of the discharge detector (DDX 7000) through a transient filter. A penetration panel is used between the test and control chamber to inhibit the passage of noise. The star earth is fed to the driver earth of the building. All the above equipment is placed in an electromagnetically shielded 'test chamber' except

for the discharge detector that is housed in an adjacent ‘control chamber’ along with other equipment used for PD analysis.

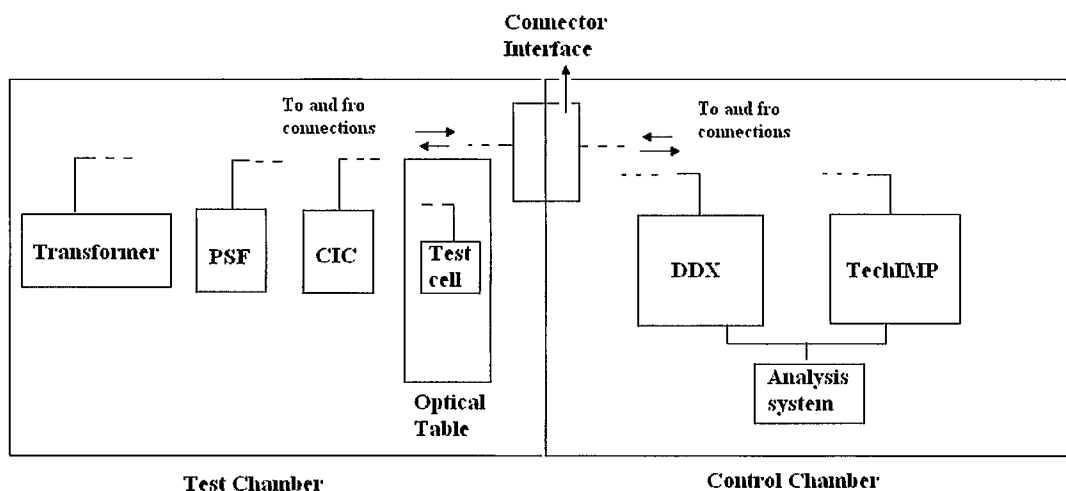


Fig. 3.3: Schematic Diagram (including layout) of the setup.

Figure 3.3 shows the layout of the instruments in the lab. The control chamber houses a control panel that controls the input voltage to the primary of HV transformer, through a PLC controlled autotransformer. The over current relays, tripping circuits, external interlocks are all used in the protection scheme. The control panel also houses a transient filter that grounds off any dangerous transients in the event of a flashover. Isolation transformers are used to block noise from entering the measuring circuitry. The discharge detector (DDX-7000) and the analysis system (TECHIMP PD check) are housed in the control chamber and the signals to and from them are passed through the transient filter and then connected to the PSF via a connector interface. Each component of the setup is described separately in the next section of this chapter.

3.4 Description of the system components

The following section describes the basic functionality and configuration of the various components of the experimental setup used for PD detection, measurement and analysis at the IDEL.

3.4.1 PD generation and measurement components

(a) Electromagnetically shielded test chamber

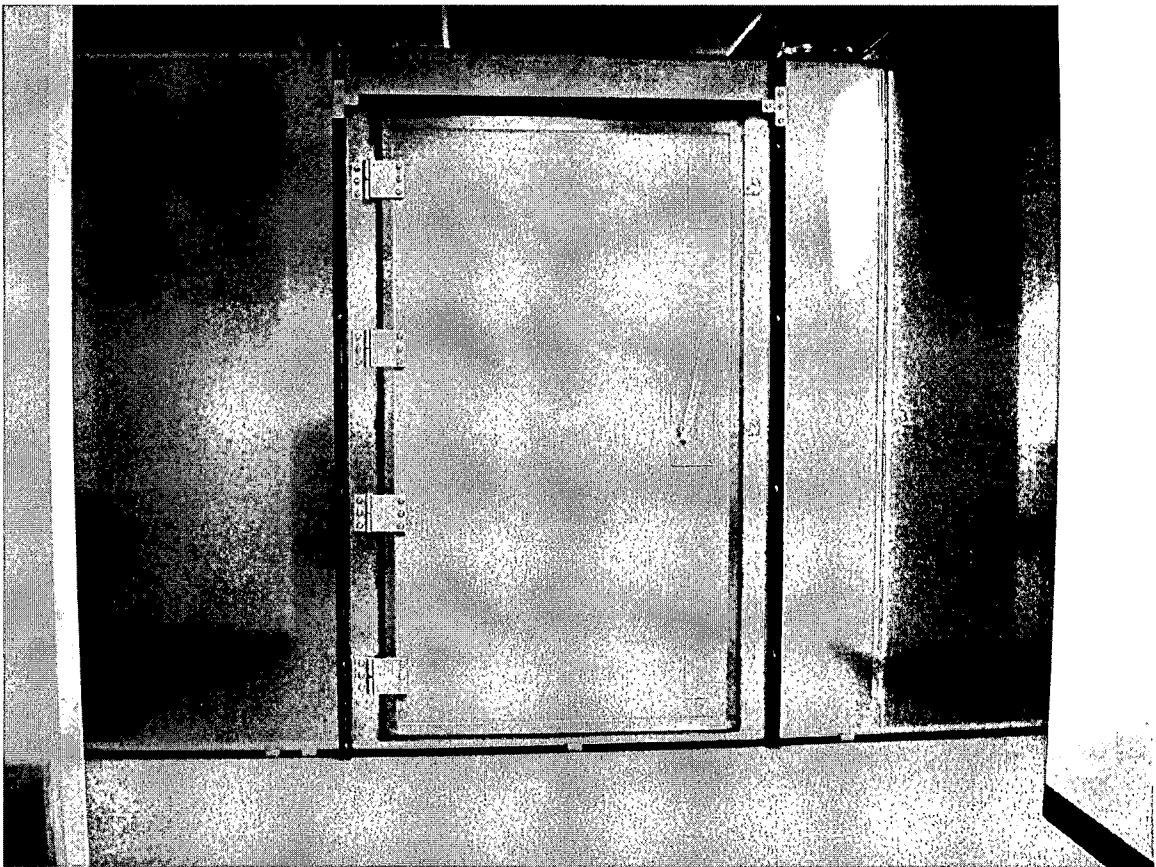


Fig.3.4: Outside of the EM Test Chamber.

The test chamber is an electromagnetically shielded room that houses the discharge free transformer (HV source), a coupling capacitor, a charge injection capacitor, a power separation filter and detecting impedance. Electromagnetic shielding is

used to block electromagnetic radiations and unwanted high frequency pulses from entering the equipment inside the chamber and to prevent any noise from creeping into the PD measurements done inside the chamber. In addition, the chamber also provides protection from the high voltage connections needed for the testing.

(b) Transformer

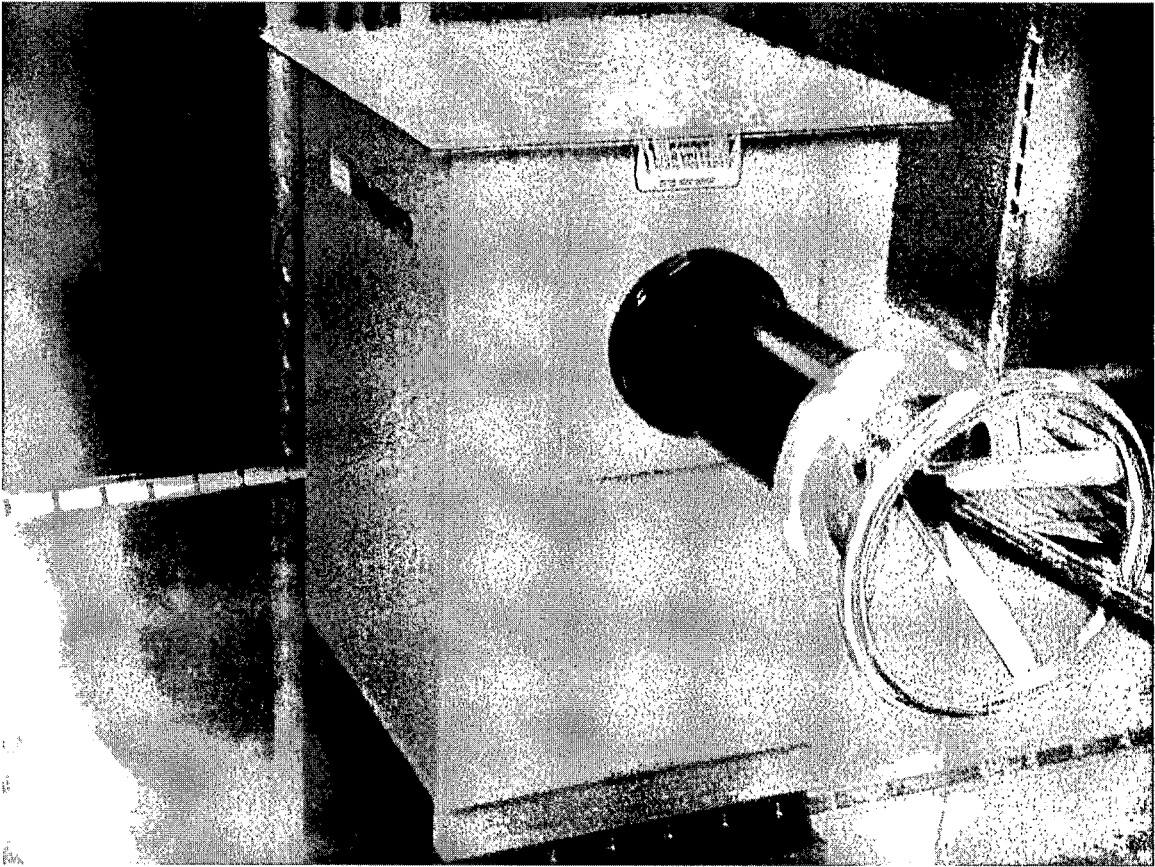


Fig.3.5: Discharge free transformer.

In order to assess the condition of the power apparatus (cables, bushings, etc.), a source that does not introduce PD into the measurements by itself is needed. It should have enough voltage range to test a variety of samples without giving rise to internal PDs from the source. Figure 3.5 shows the discharge free transformer used at IEDL as the ac power source. It is a 250V/100 kV, 10 kVA, 60 Hz PD free transformer.

(c) Power separation filter (PSF)



Fig.3.6: Power Separation Filter.

In high voltage circuits, the power separation filter (PSF) is used for a PD free connection that splits the voltage between the coupling capacitor and the detecting impedance. The PSF is connected in series with a 'quadrapole' that consists of detecting impedance and a matching unit and all of these constitute a PSF unit as shown in Figure 3.6. A coupling capacitor is used in order to drop most of the applied voltage across it while feeding only the high frequency pulses across the detecting impedance. Detecting impedance is used here to convert the sharp rise time PD pulse into a damped sine wave. The damped PD pulse is rectified and is measured by the discharge detector. It is

desirable to have a RLC or RC detecting impedance whose characteristics match with those of the discharge detector. A matching unit is used in order to adjust the magnitude of the RLC such that it gives the requisite value of the impedance to suit the input characteristics of the discharge detector. The PSF at IEDL is rated as 1nF at 100 kV.

(d) Charge injection capacitor (CIC)

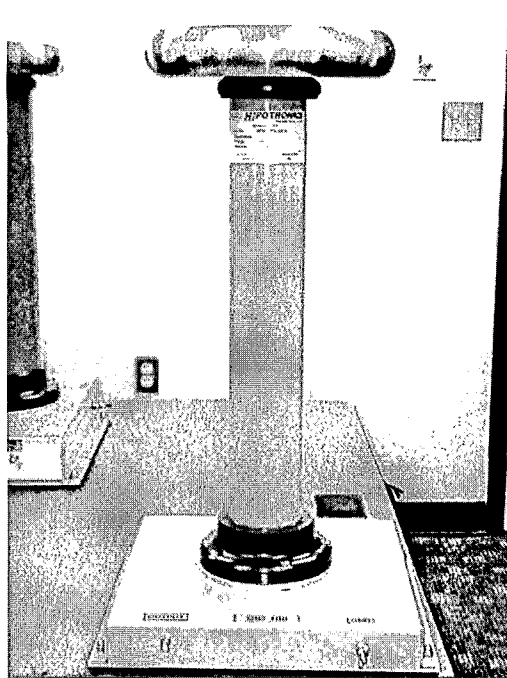


Fig.3.7: Charge injection capacitor.

In order to measure the magnitude of the pulses coming from the sample under test, a reference pulse of known charge magnitude must be generated to compare against the incoming pulse from the sample. A PD system must come with this calibration pulse generator system to achieve calibration. A calibrating pulse generator feeds a known amount of charge to the Charge Injection Capacitor (CIC) in order to get a reference measure for incoming PDs. The CIC at IEDL has a capacitance of 0.1 nF, and is rated at 100 kV.

(e) Test cell

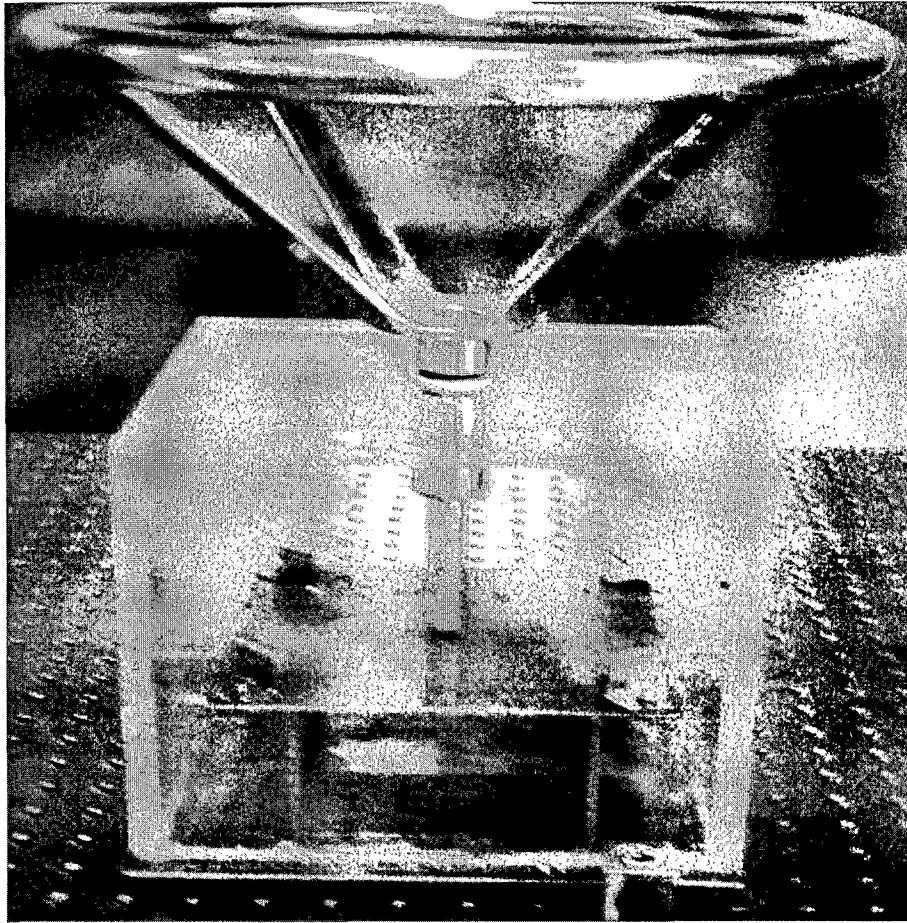


Fig.3.8: Test Cell.

The test cell unit houses the test sample for which PD are to be detected and measured. The test cell must contain an appropriate electrode system that only produces discharges within the test sample. Corona free rings are used to make discharge free high voltage connections. The connections to the test cell are made through a 1¼" polished copper tube. The cell has a HV electrode and a ground electrode. The ground electrode is connected to a star point earth using two AWG cables. The test cell is made of plexiglass

for observing any visible discharge phenomenon and is mounted on an optical table to enable microphotography of the sample, if necessary.

3.4.2 The PD analysis system components

(a) The control chamber

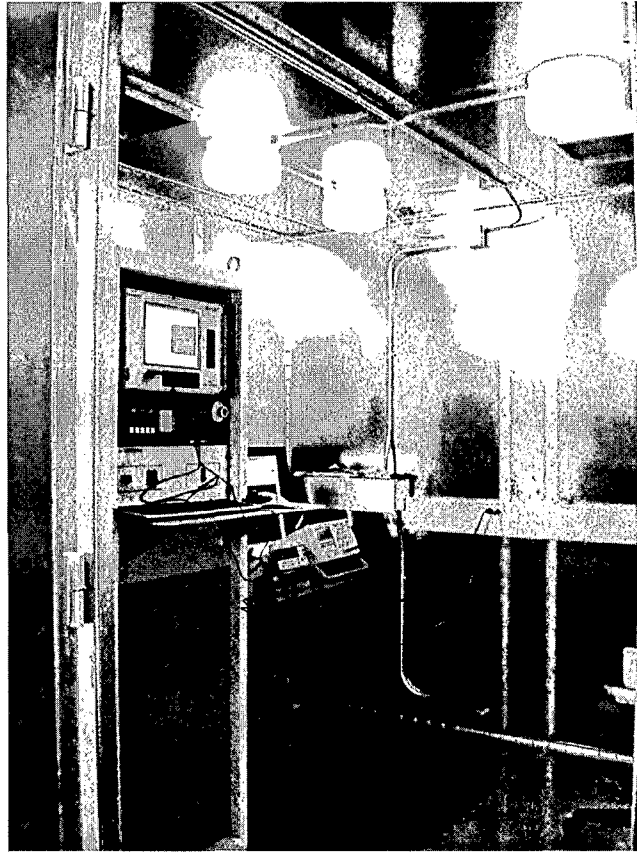


Fig.3.9: Complete view of the control chamber of PD measurement set up.

A control room is used to remotely observe the PD measuring system, control the voltage applied to the sample, and acquire the PD data for pulse height and phase analysis. The computer systems in the control room are also used for analysis of the PD data to obtain useful diagnostic information about the status of the insulation system.

(b) Discharge detector

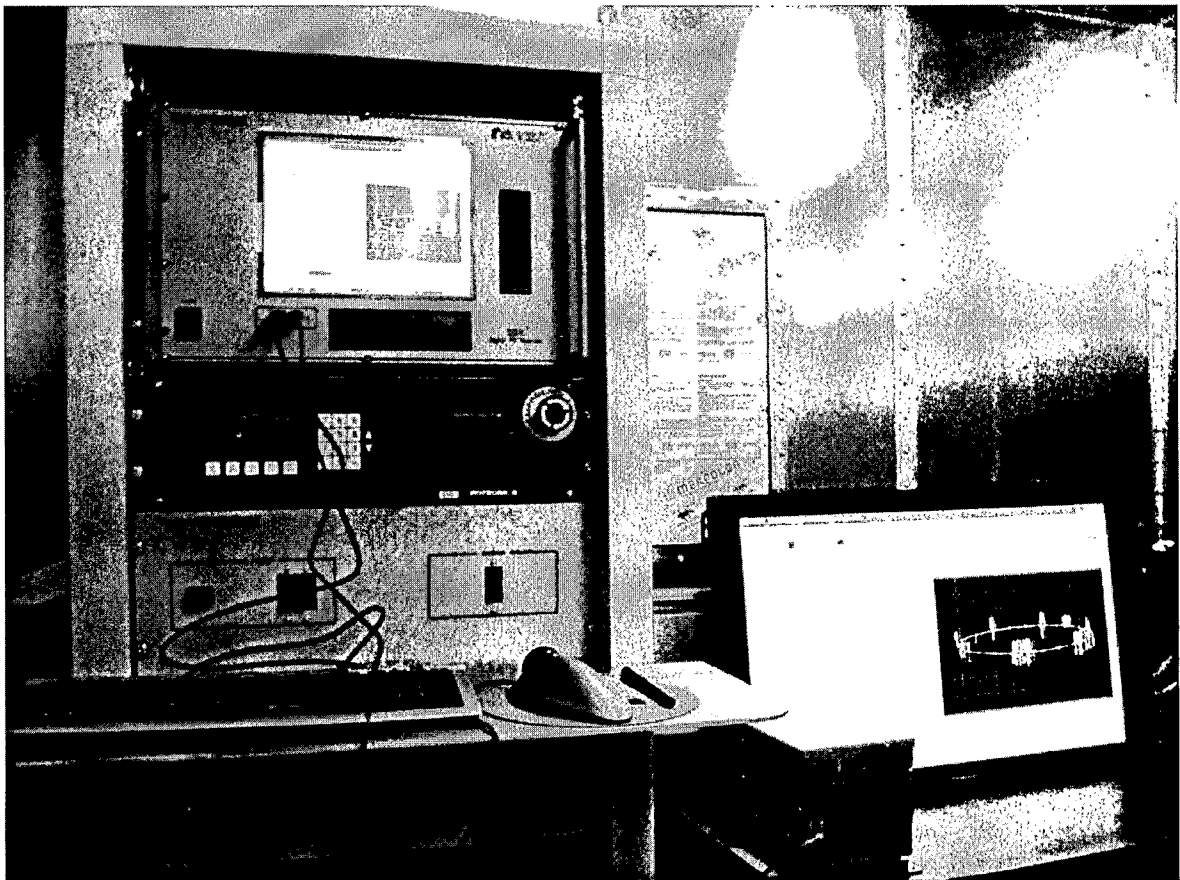


Fig.3.10: The control panel of the DDX-7000 Discharge Detector.

The discharge detector takes the damped oscillations from the detecting impedance, rectifies and integrates the pulse and then feeds it into a pre-amplifier and amplifier to bring the output pulse to a level that can be observed on an oscilloscope screen.

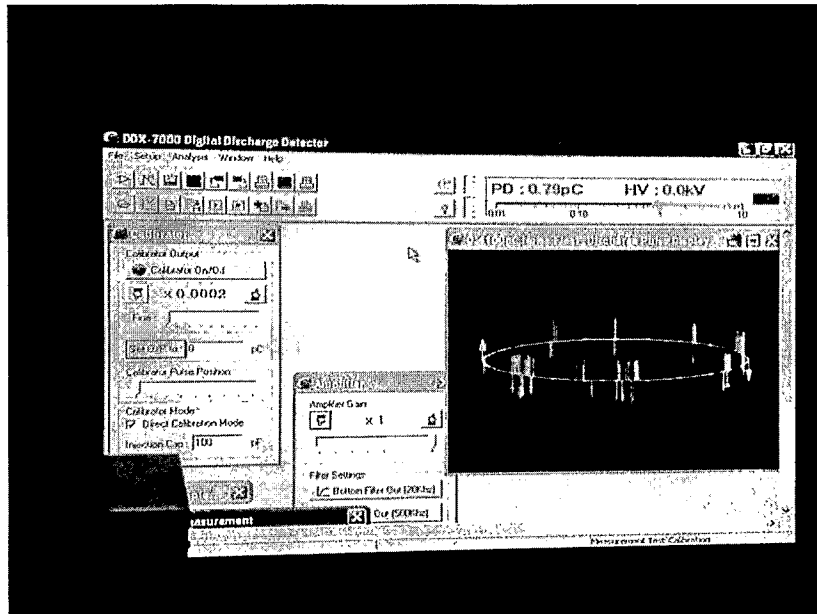


Fig 3.11: A shot of the front panel of the DDX detector software which displays the automatics calibrator and PD elliptical pulse display.

The output pulses can be displayed on an elliptical time base that shows the pulse occurrence location in 360 degrees (as shown in Figure 3.11), or on a regular time base. The criteria used for selecting a PD detector system are sensitivity (in picocoulombs), reference pulse generation, and the ability to obtain an auxiliary output to feed it into pulse height analyzers or pulse phase analyzers for further analysis. The discharge detector used at IEDL is the Hippotronics DDX-7000 that is a fast and reliable piece of automated PD detecting and testing equipment. It has several features such as automatic calibration, real-time pulse display and measurement and test report generation that makes it an ideal choice for the use of detection of PD pulses (Ref [33]).

(c) TECHIMP PD check system

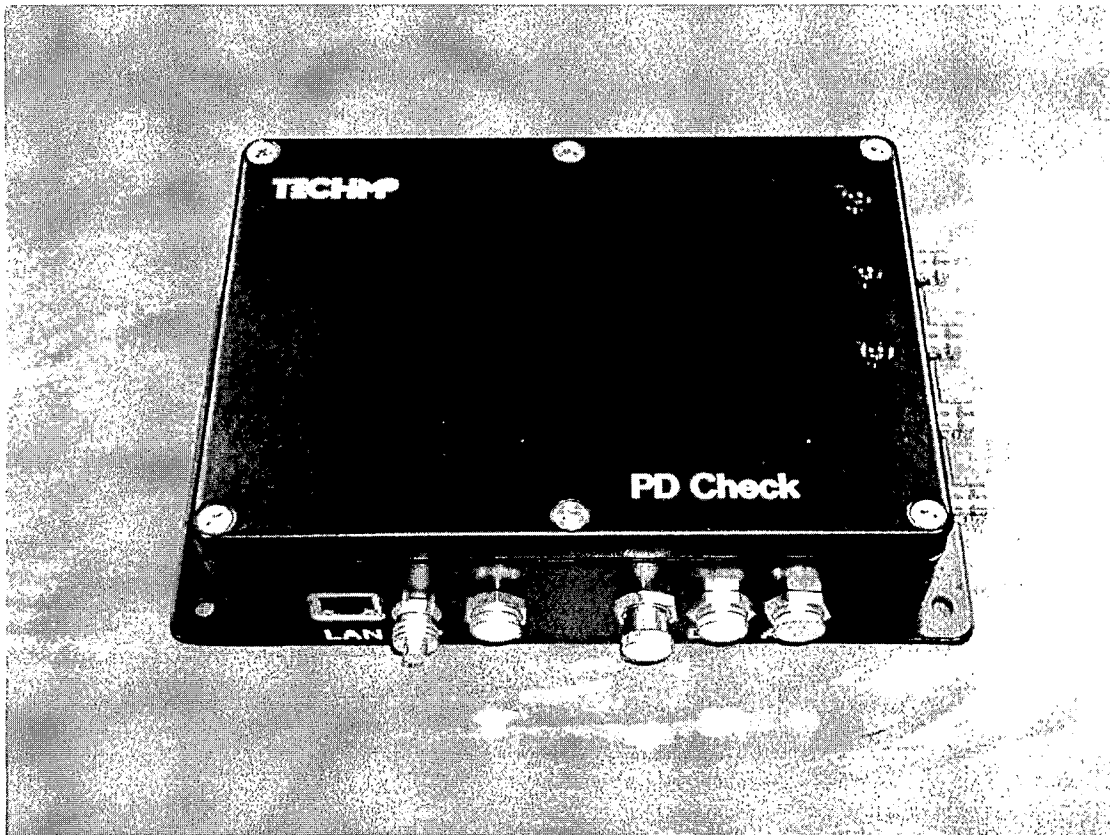


Fig.3.12: PD measurement system from Italian company TECHIMP.

The TECHIMP PD check is an efficient PD analysis system that provides condition assessment of high voltage and medium voltage systems based on PD detection. PD check has the capability to perform pulse height, pulse phase and pulse sequence analysis. It is driven by national instruments (NI) hardware and software and new user-defined modules can be added to it. It allows real-time data to flow from the TECHIMP system to a monitoring PC and also provides noise rejection to provide better signal analysis and visualization (Ref [34]).

CHAPTER 4

RESULTS AND DISCUSSIONS

In this chapter the simulation results for prediction of the PD pulse height parameters are presented. Two different approaches -- a linear prediction technique using MATLAB and an artificial neural network model -- have been used for forecasting the future values of the shape and scale parameters. The input data used for both methods were the results of the shape and scale parameters obtained from the experimental setup as was described in chapter 2.

4.1 Prediction of parameters using linear prediction method

Prediction of any data by a model like linear prediction or artificial neural networks is basically a two step process. The first step is to train the model by breaking the existing data into two parts, 'input' and 'output', and then feeding the input part of the data to the model, observing its predicted output, and comparing it to the output part of the existing data. The training is done so that the model can understand the nature, behavior and trends or fluctuations in that data and come up with its own function to forecast the future values of that data. A model is successfully trained once the output obtained from the model provides minimal mean square error when compared to the calculated mean square error of the output part of the existing data. Mean square error (MSE) is a good estimator of the accuracy of a prediction model as it quantifies the amount by which an estimator differs from the correct value of the quantity that is being estimated. MSE is basically calculated as the second moment of the error (the difference

between the predicted value and the existing value). A prediction model is efficient if the MSE obtained from its estimated output is close to the mean square error calculated on the existing data. The next step after training is to then observe the predicted output of the model for different sets of input data and measure its mean square error to determine its efficiency.

The linear prediction model used to forecast the PD shape and scale pulse height parameters as presented in chapter 2 was simulated using MATLAB version 7.5. First, the shape and scale parameters of both samples 'A' and 'B' of the experimental data were separated using the Weibull distribution

$$F(v_i) = 1 - (e^{-(v_i / \sigma)^\eta}) \quad (4-1)$$

where 'σ' is the scale parameters, and 'η' is the shape parameters of the data.

Sample A provided 37 points of data and sample B had 41 points of data. Then each of the shape and scale parameters were separated into their deterministic and stochastic parts. All the data was stored in 2 arrays, an input data array and an output array, to which the predicted values will be compared in order to train the model developed. The sample A shape and scale parameters had input array of 32 points, and the next 5 points were the output array. Similarly, sample B's shape and scale parameters had an input array of 36 points and the next 5 points as the output array.

The linear prediction filter is constructed using the equation

$$y[n] = e[n] - \sum_{k=1}^p (b_k y[n - k]) \quad (4-2)$$

where $y[n]$ is the obtained 'n' element array of predicted values, $e[n]$ is the prediction error in calculation, $y[n-k]$ is the k^{th} past value of the data, and b_k is the corresponding

predictor coefficient and p is the order of the filter. Therefore, in order to construct the filter, we need to find the order of the filter and its predictor coefficients first.

To find the correct order of the linear prediction filter, a part of the input array was provided to the MATLAB inbuilt function 'lpc()' with a chosen order (starting from 1). The function 'lpc()' determines the coefficients of a forward linear predictor by minimizing the prediction error in the least squares sense. The obtaining array was then compared to the actual output array stored. Through trial and error, it was observed that the sixth ordered filter gave values that were nearest to the given data. Hence, the set of predictor coefficients were obtained for a *sixth* order linear prediction filter. The second step was to provide all of the input data to the correlation filter built using equation (4-2) with the obtained predictor coefficients in order to obtain the predicted output array. This array was then compared to the actual output array and mean square error was calculated. This process was repeated for the shape and scale parameters of both samples A and B. Figures 4.1 to 4.4 show the results of the fitted linear prediction model in predicting the shape and sigma parameters for the two different samples. In all the figures, filled circles represent predicted value and unfilled circles show the actual value. The least means square errors (MSE) achieved by the model for that set of data is also shown along with the calculated means square error of the existing data denoted by $(MSE)_p$.

Figure 4.1 shows the prediction performance for the shape parameter of sample A. The prediction was done for all the 37 points of data. The predicted mean square error $(MSE)_p$ calculated for the data was 0.0819. The mean square error (MSE) achieved in prediction was 0.0890.

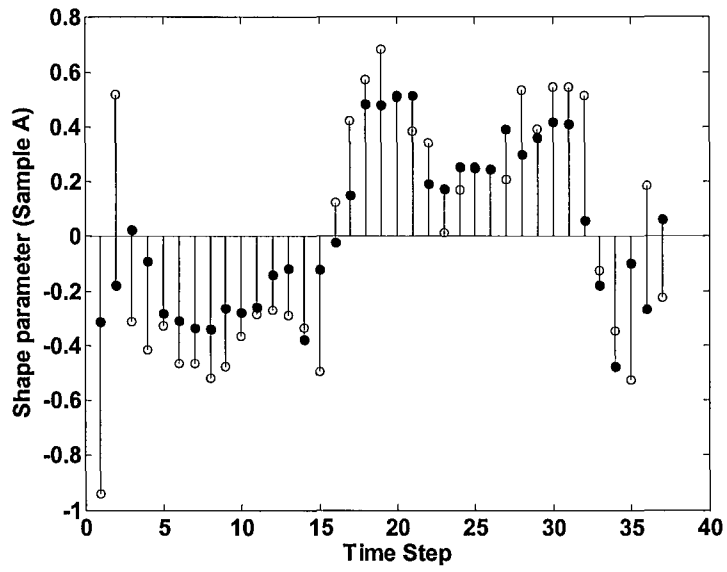


Fig 4.1: Prediction performance for shape parameter of sample A.

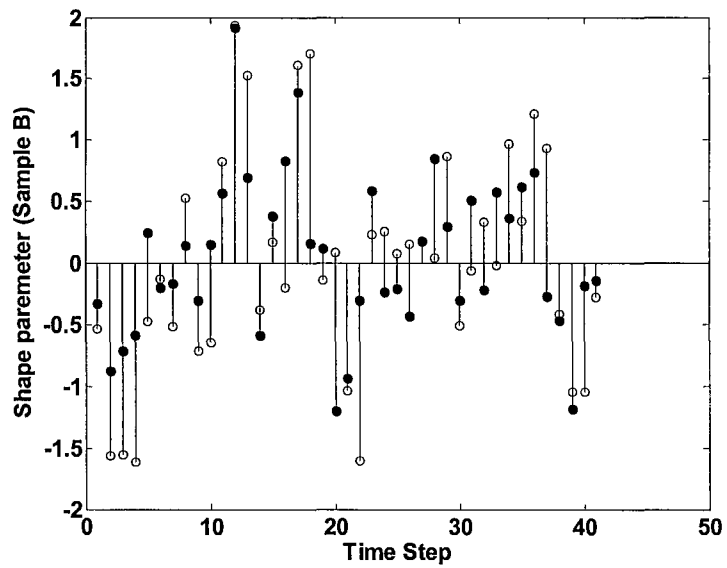


Fig 4.2: Prediction performance for shape parameter of sample B.

Figure 4.2 shows the prediction performance for the shape parameter of sample B. In the figure, filled circles show predicted value and unfilled circles show actual value. The prediction was done for all the 41 points of data. $(MSE)_p$ calculated for the data was 0.0802. The MSE achieved in prediction was 0.4095.

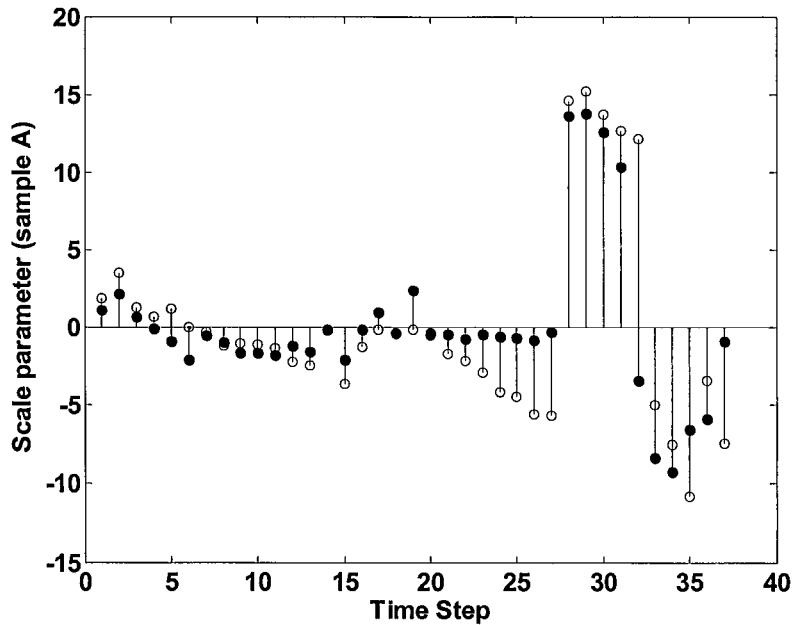


Fig.4.3: Prediction performance for scale parameter of sample A.

Figure 4.3 shows the prediction performance for the scale parameter of sample A. $(MSE)_p$ calculated for the data was 20.6197. The MSE achieved in prediction was 24.9675. Figure 4.4 shows the prediction performance for the shape parameter of sample B. $(MSE)_p$ calculated for the data was 25.4310. MSE achieved in prediction was 30.4318.

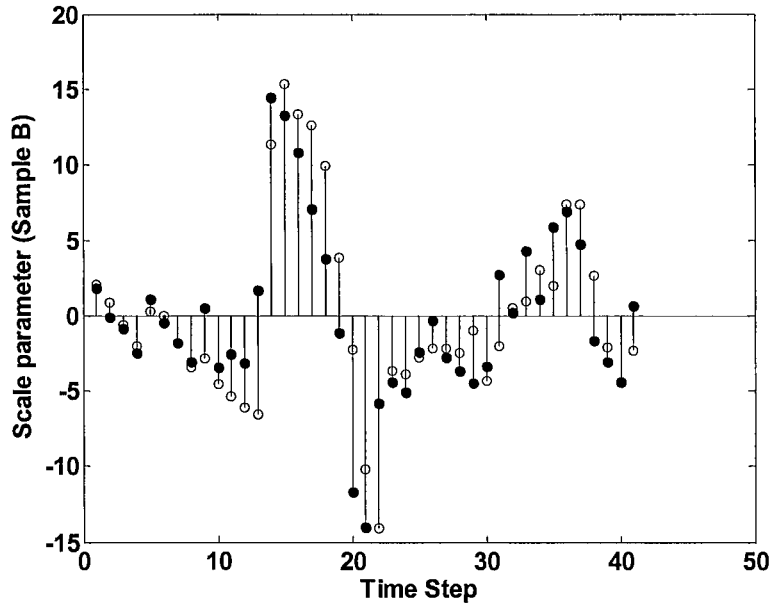


Fig.4.4: Prediction performance for scale parameter of sample B.

From the plots, it was observed that the MSE for scale and shape parameters of both samples was very close to the $(MSE)_p$, which means that prediction occurred with reasonable accuracy. In general, the linear prediction filter can predict up to 6 future values of the shape and scale parameters of the PD data with reasonable mean square error.

4.2 Prediction of parameters using artificial neural networks

The linear prediction filters can be used to predict only the stochastic portions of both the parameters successfully. Also, although mean square errors for the shape parameters of the linear prediction model were as expected, the MSE for scale parameters could have been closer to the calculated value. Since the shape and scale parameters of

PD data are essentially a pair of time series, it was observed that artificial neural network techniques could be applied for their forecasting. As explained in chapter 2, a recurrent Elman network with a sigmoidal first layer and a linear second layer was used for prediction in this method. The network was simulated using MATLAB version 7.5. The first part of the simulation was the same as the simulation for linear prediction – the shape and scale parameters of both samples were divided into input and output arrays for both samples. The input arrays for sample A and B contained 32 and 36 elements each, and for both samples the output arrays contained 5 points each.

An Elman network has connections from its second layer back to the first layer. Because of this, the function, which is learned by this network, can be based on the current inputs plus an array of the previous outputs of the network. With proper training, the network is able to learn any prediction from the combination on inputs and stored outputs to provide future values of that system. MATLAB software has a complete ‘neural network toolbox’ that contains a lot of inbuilt functions that helped to develop and train the Elman network very efficiently. The function ‘newff()’ was used to create the recurrent network. The functions ‘purelin()’ and ‘tansig ()’ were used to construct the first sigmoidal layer and second linear layer. The developed network was trained for different combinations of values of the input array combined with the output array with varied number of neurons to obtain the predicted results. The process was repeated for the shape and scale parameters of both samples. It was observed that the network trains well when its neurons range from 10 to 30 in number.

Figures 4.5 to 4.9 show the results of the recurrent Elman Network in predicting the shape and sigma parameters for two different samples. For all the figures, filled

circles show predicted value and unfilled circles show actual value. Thirty data points were used for prediction. It can be seen from these results, that prediction of up to 10 future values can be done with reasonable accuracy for both samples.

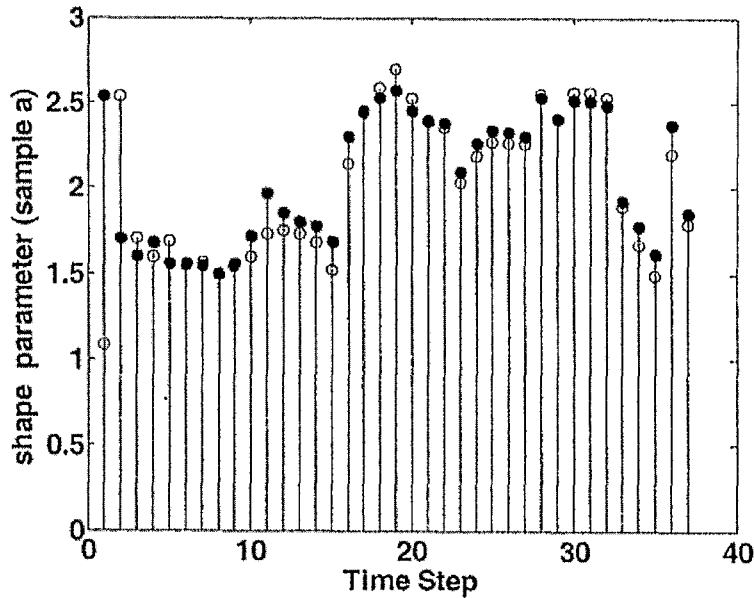


Fig.4.5: Prediction performance with 10 neurons.

Figure 4.5 shows the prediction results of the shape parameter of sample A for 10 neurons. $(MSE)_p$ calculated for the data was 0.0819. The mean square error achieved was 0.0788. Figure 4.6 shows the prediction results of the shape parameter of sample A for 30 neurons. $(MSE)_p$ calculated for the data was 0.0819. The mean square error achieved was 0.0842.

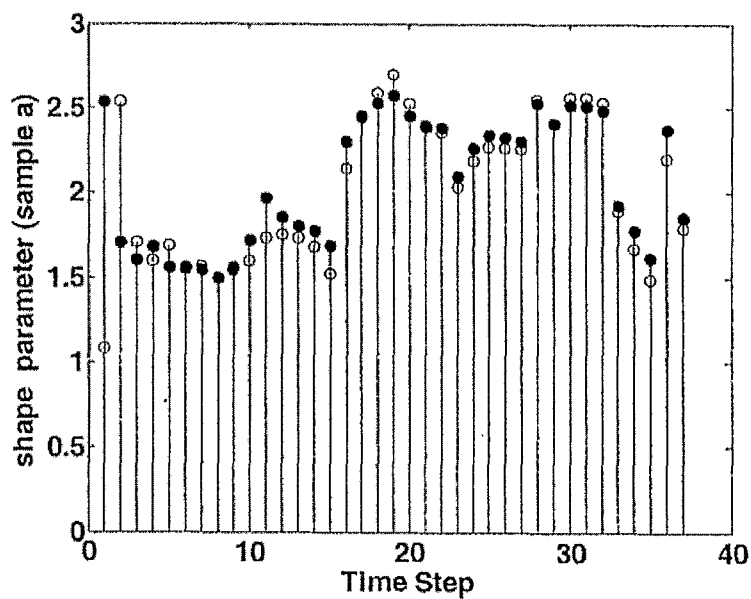


Fig.4.6: Prediction performance with 30 neurons for shape parameter.

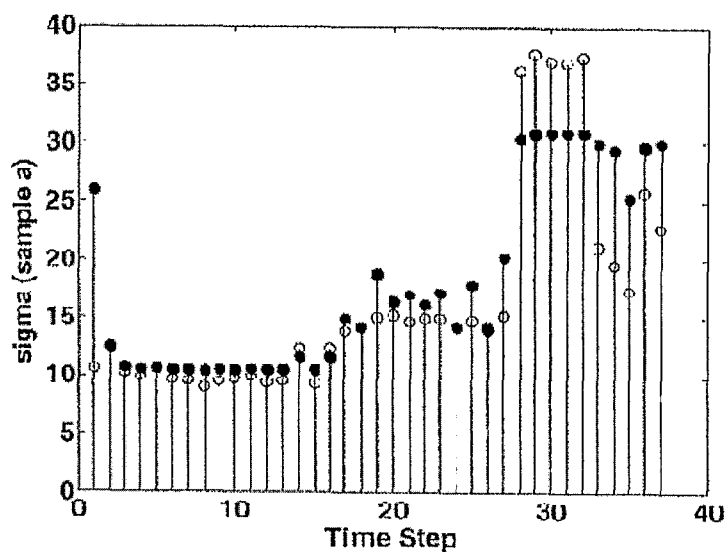


Fig.4.7: Prediction performance with 30 neurons for scale parameter.

Figure 4.7 shows the prediction results of the scale parameter of sample A for 30 neurons. $(MSE)_p$ calculated for the data was 20.6197. The mean square error achieved was 22.0958.

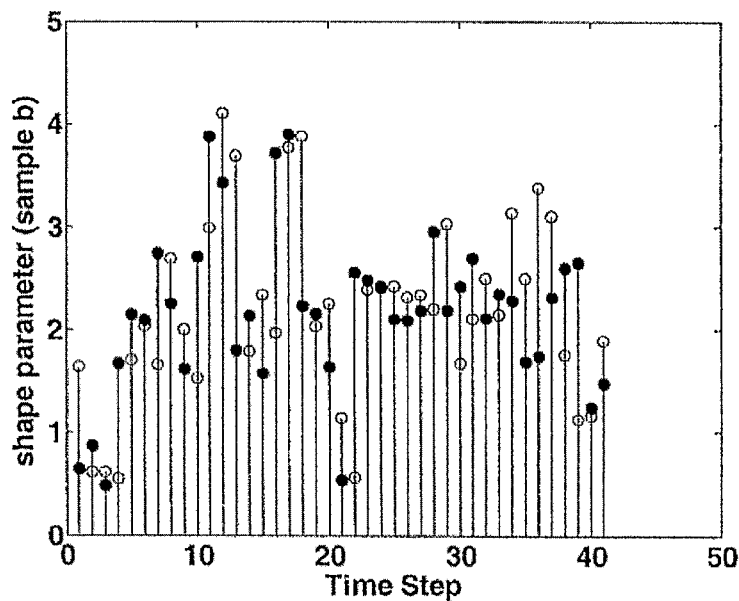


Fig.4.8: Prediction performance with 22 neurons.

Figure 4.8 shows the prediction results of the shape parameter of sample B for 22 neurons. $(MSE)_p$ calculated for the data was 0.0802. The MSE achieved was 0.0982. Figure 4.9 shows the prediction results of the scale parameter of sample B for 24 neurons. $(MSE)_p$ calculated for the data was 2534310. The MSE achieved was 26.4529.

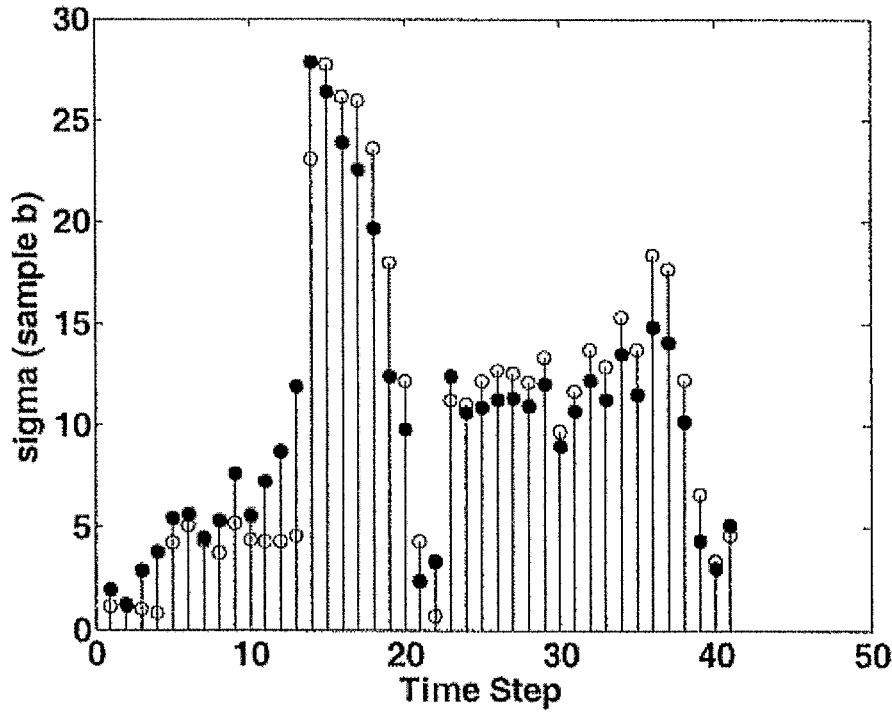


Fig.4.9: Prediction performance with 24 neurons.

From the plots, it can be observed that the MSE obtained by the ANN technique for both scale and shape parameters was closer to $(MSE)_p$ than the earlier technique. This shows that this method appears to be more accurate in predicting the PD pulse height parameters. The neural networks model is able to predict up to the next 10 values of the data with good accuracy.

4.3 Comparison of the two techniques

Table 4.1 compares the Mean square errors obtained by prediction of stochastic variations of shape and scale parameters by different methods.

Table 4.1
Comparison of means square errors of both methods

Method	Shape Parameter (Sample A)	Shape Parameter (Sample B)	Scale Parameter (Sample A)	Scale Parameter (Sample B)
Linear prediction	0.0890	0.4095	24.86751	30.4318
Artificial neural networks	0.0788	0.0982	22.0958	26.4529

Observations made from the results of the two prediction techniques are summarized as follows:

- 1) From the table, it can be observed that the artificial neural networks gave the least mean square errors overall for both shape and scale parameters of samples A and B as compared to the linear prediction method.
- 2) The artificial neural networks can be used to predict both the deterministic and stochastic portions of the PD data, but the linear prediction filters can be used to predict only the stochastic portions of both the parameters.
- 3) The choice of the order of the linear prediction filter is probabilistic and is obtained through trial and error; it may be difficult to obtain the correct order of the filter when a large amount of data is being predicted.

- 4) It is easier to code the artificial neural networks model in one monolithic MATLAB program; the construction of the linear prediction filter requires more than one program.
- 5) The neural networks model is able to predict up to the next 10 values of a 40 point PD data with reasonable accuracy whereas the linear prediction filter could predict only up to 6 future values of the same data.

In conclusion, it can be stated that the artificial neural networks are more efficient in predicting the partial discharge pulse height distribution parameters. Linear prediction filters should be used only if there is a need to determine the trend of the stochastic portions of the pulse height parameters. If the artificial neural network is developed with more layers and trained, it can predict a large amount of PD data with good accuracy.

CHAPTER 5

CONCLUSIONS AND FUTURE WORK

5.1 Conclusions of the thesis

Linear prediction and artificial neural networks have been used to analyze and predict the pulse height distribution parameters of a set of partial discharge data in this work. In the linear prediction technique the covariance and auto covariance formulation are solved to find the best fitting predictor coefficients for the given data. In the artificial neural network technique, an ‘Elman network’ which is a two layer recurrent network- with a sigmoidal first layer and a linear second layer, was used to build the prediction model. Both the techniques were simulated in MATLAB with the shape and scale- pulse height parameters obtained from an earlier work of two PMMA samples. Simulation results show that both the methods predict the future values of each sample with optimal mean square errors. A comparison of the two methods suggests that overall the neural network model was more accurate in predicting the future values of the shape and scale parameters of both the samples, and the linear prediction model can be used to predict the stochastic part of the pulse height distribution parameters of any given data.

5.2 Future work

(1) A digital acquisition system is being developed that can measure phase ‘ ϕ ’ and apparent charge ‘ q ’ values of ‘ n ’ number of PD’s occurring on a given power line voltage and then plot a 3D $n(\phi, q)$ that would completely characterize the set of PDs. The system is developed using a fast Digitizer Card NI- 5112, which is a 2-channel high speed card (100 MS/s) with acquisition and analyses programs written in LabVIEW 8.2.

The system is being tested using artificially generated PD pulses that have variable ' ϕ ' and ' q ' magnitudes, and their performance is benchmarked by comparing the resulting plots with the plots obtained by processing the same data on the existing PD analysis system called TECHIMP- PD check, (Ref [34, 35]).

(2) Research will continue on acquisition, analysis and prediction of PD data with reference to electrical tree growth in various materials such as cross linked polyethylene, epoxy, PMMA, etc.

(3) As a part of the 'VAMAS' project, which is an international consortium of scientists, I will be investigating the effect of nano- fillers on the partial discharge characteristics in polypropylene films.

(4) The linear prediction and neural network techniques that have been implemented in MATLAB (Ref. [25, 26]) have shown great promise in analyzing and forecasting PD pulse patterns. These algorithms will be coded in LabVIEW, or an interface will be built between the LabVIEW program (used in TECHIMP) and the MATLAB code that has been developed. Currently, the PD check uses the LabVIEW environment to acquire and analyze the data. Hence, integrating these modules with the existing program will greatly enhance the PD acquisition and analysis capability of PD check and allow us to acquire and analyze data in real time.

REFERENCES

- [1] F. H. Kreuger, *Partial Discharge Detection in High-Voltage Equipment*, Temple Press, Butterworths, 1989.
- [2] J. H. Mason, "Discharge detection and measurements", *Proc Inst Electrical Eng*, 112, 7, pp. 1407-1423, 1965.
- [3] D. Kind and D. Konig, "AC Breakdown of Epoxy Resins by Partial Discharges in Voids", *Electrical Insulation, IEEE Transactions on Dielectrics and Electrical Insulation*, Volume EI-3, Issue 2, pp. 40 – 46, May 1968.
- [4] L. Centurioni, G. Coletti, and F. Guastavino, "An experimental study to investigate the effects of partial discharges (PD), of electric field and of relative humidity during surface PD tests on thin polymer films" , *Electrical Insulation and Dielectric Phenomena*, pp.239 - 242 vol.1, 17-20 Oct. 1999.
- [5] A.S Pillai and U.C Trivedi, "Aging effect on partial discharge values and electrical performance of XLPE cable" *Electrical Insulation, Conference Record of the 1988*, pp.211 – 214, 1988.
- [6] A.C. Gjaerde," The combined effect of partial discharges and temperature on void surfaces" *Electrical Insulation and Dielectric Phenomena, 1997. IEEE 1997 Annual Report*, Volume 2, pp. 550 – 553, 19-22 Oct. 1997.
- [7] K. Chrzan, and J. M. Andino, " Electrical strength of air containing ozone and nitric oxides produced by intensive partial discharges, *Electrical Insulation* ,Volume 8, Issue 4, pp. 607 - 611, Aug. 2001.
- [8] J. Makhoul, "Linear Prediction: A tutorial Review", *Proc. IEEE*, Vol. 63, pp. 561-580, 1975.
- [9] G.C. Montanari, A. Contin, and A. Cavallini, "Random sampling and data processing for PD-pulse height and shape analysis " *IEEE transactions on Dielectrics and electrical insulation*, vol.7, no.1, pp. 30-39, 2000.
- [10] R. Bartnikas and E. J. McMahon, *Engineering Dielectrics I - Corona Measurement and Interpretation, Astm Intl*, 1979.
- [11] E.Kuffel and W.S. Zaengl, *High Voltage Engineering Fundamentals*, Pergamon Press. First edition, 1992.
- [12] E.Kuffel, M.Abdullah, and W.S. Zaengl, *High Voltage Engineering*, Pergamon Press. First edition, 1970.

- [13] M. Hoof and R. Patsch, "Analyzing Partial Discharge Pulse Sequences – A New Approach to Investigate Degradation Phenomena." *ISEI'94*, Pittsburgh, USA, pp. 327-31, 1994.
- [14] J. Austin and R. E. James, "On-line Digital Computer System for Measurement of Partial Discharges in Insulation Structures", *IEEE Trans. Elec. Insulation.*, Vol. 11, No. 4, pp. 129-139, December 1976.
- [15] T. Tanaka and T. Okamoto, "A Minicomputer Based Partial Discharge Measurement System", *IEEE Int. Symp on Electrical Insulation*, pp. 86-89, June 1978.
- [16] E. Gulski and F. H. Kreuger, "Digital Computer System for Measurement of Partial Discharges in Insulation Structures", *3rd Int. Conf. on Conduction and Breakdown in Solid Dielectrics, Trondheim*, pp. 582-586, 1989.
- [17] E. Lemke, T. Strehl, and H. Elze, *Advanced measuring system for complex analysis of dielectric Parameters and PD phenomenon*, Lemke Diagnostics, Volkersdorf, Germany, 1999.
- [18] R. E. James and B. T. Phung, "Development of Computer-based Measurements and their Application to PD Pattern Analysis ", *IEEE transactions on dielectrics and Electric Insulation*, Vol. 2, No. 5, pp. 838-856, 1995.
- [19] Z. Berler, A. Golubev, A. Romashkov, and I. Blokhintsev, "A New Method of Partial Discharge Measurements", *CEIDP-98 Conference*, Atlanta, GA, October 25-28, 1998.
- [20] A. Lapp and H.G Kranz, "The use of the CIGRE data format for PD diagnosis applications", *IEEE Trans on Dielectric Insulation*, pp. 102–112, 2000.
- [21] S.S. Kumar, "PD data analysis and evaluation of partial discharge patterns for uniform characterization". *Proc. 12th Int. Symp. on High-voltage Engineering*, Bangalore, India, pp. 1047–1050, August 2001.
- [22] R. Patsch, and F. Berton, "Pulse-Sequence-Analysis - Chances to Characterize Defects." *CEIDP'99*, Austin, Texas, USA, pp. 243-2488, 1999.
- [23] P. Basappa and V. Lakdawala, "Application of Digital Signal Processing Techniques to Analyze Partial Discharge Data", *IEEE-CEIDP - 2000*, pp. 341-346, October 2000.
- [24] P. Basappa and V. Lakdawala, "Statistical analysis of Partial Discharge data evolved during tree growth", *IEEE-CEIDP - 2001*, pp. 361-364, October 2001.
- [25] V. Nimbole, V. Lakdawala, and P. Basappa, "Prediction of Partial Discharge Pulse Height Distribution Parameters using Linear Prediction Method ", *Electrical Insulation and Dielectric Phenomena, CEIDP 2008*, pp.337 – 340, 26-29 Oct. 2008.

- [26] M. M. Noel, P. Basappa, V. Lakdawala and V. Nimbole, "A Neural Network based System for prediction of Partial Discharge Pulse Height Distribution Parameters", *Conference Record, IEEE - ISEI -2008*, pp.331-335, June 2008.
- [27] G.J Hahn and S.S Shapiro, *Statistical Models in Engineering*, John Wiley and Sons, 1967.
- [28] N.P Kolev, E.D Gadjeva, M.G Danikas, and N.R Gourov," An approach to develop a partial discharge investigation" *Electrical Insulation Conference and Electrical Manufacturing & Coil Winding Conference*, pp. 507-510, 1999.
- [29] N. Singh, O.E Morel, S.K Singh, and T. Rodenbaugh ,“The assessment of the degree of paper aging and remaining life of fluid-filled paper-insulated high voltage underground transmission cables through wet-tensile strength”, *Electrical Insulation*, Volume 8, Issue 4, pp. 607 – 611, Aug. 2001.
- [30] S. Haykin, *Neural Networks: A Comprehensive Foundation*, Prentice Hall, 2nd edition, 1998.
- [31] Hippotronics’ Discharge detectors User’s Guide.
- [32] PSF & CIC brochure.
- [33] DDX 7000/8003 brochure.
- [34] TECHIMP PD Check Users manual.
- [35] A. Jambula, V. Nimbole, V. Lakdawala, and P. Basappa,” Development of a Digital Acquisition System for Partial Discharge Measurement and Analyses *Electrical Insulation Conference, EIC 2009*, pp.60 – 63, 2009.

VINAY N. NIMBOLE

Department of Electrical and Computer Engineering
Old Dominion University, Norfolk, VA- 23508.
Contact: (919)-986-2053
Email: vnimb001@odu.edu

EDUCATION

Master of Science in Electrical and Computer Engineering (Fall'09) from Old Dominion University, Norfolk, VA (GPA of 3.75).

Bachelor of Science in Electronics and Communications Engineering (Fall'06) from Jawaharlal Nehru Technological University, Hyderabad, India (GPA of 3.75).

RELATED EXPERIENCE

- Teaching Assistant, Department of Electrical and Computer Engineering, Old Dominion University, Norfolk, VA, (Jan'08 – June'09).
- Project Associate during ,NEO Power projects Ltd, Mumbai, India (Dec'06- June'07)
- Process Associate, General Electric, Hyderabad, India. (Feb'05- Aug'06)

RESEARCH PUBLICATIONS

- V. Nimbole, A. Jambula, V. Lakdawala, P. Basappa ,” *Development of a digital acquisition system for partial discharge measurement and analyses* ”, **Electrical Insulation Conference, EIC 2009**. Page(s):60 – 63, 31 May -3 June. 2009.
- V. Nimbole, V. Lakdawala, P. Basappa ,” *Prediction of Partial Discharge Pulse Height Distribution Parameters using Linear Prediction Method* ”, **Electrical Insulation and Dielectric Phenomena, 2008. CEIDP 2008**. Page(s):337 – 340, 26-29 Oct. 2008.
- V. Nimbole, P. Basappa, V. Lakdawala and M. M. Noel, "A Neural Network based System for prediction of Partial Discharge Pulse Height Distribution Parameters", **Electrical Insulation 2008, IEEE - ISEI -2008**, Page(s):331-335, June 2008.

PROFESSIONAL ACHIEVEMENTS

- Successfully presented three conference papers (EIC 2009, CIEDP 2008 and IEEE- ISEI 2008).
- Member of IEEE Association, Mahatma Gandhi Institute of Technology, Hyderabad, India.
- Volunteer for The National Service Scheme (a social services organization in India).
- School captain for the year 1999-2000 at Vidya Dayini Model High School, Hyderabad, India.